FINAL REPORT

for

CHARACTERIZATION OF RECOMBINATION AND CONTROL
ELECTRODES FOR SPACECRAFT NICKEL-CADMIUM CELLS

JUNE 9, 1966 to JUNE 9, 1967

CONTRACT NO.:   NAS 5-10241

Prepared By

GULTON INDUSTRIES, INC.
Alkaline Battery Division
212 Durham Avenue
Metuchen, N. J.

for

GODDARD SPACE FLIGHT CENTER
Greenbelt, Maryland

FACILITY FORM 602

(ACCESSION NUMBER)

(PAGES)

(NASA CR OR TMX OR AD NUMBER)

(THRU)

(CODE)

(CATEGORY)

FINAL REPORT

for

CHARACTERIZATION OF RECOMBINATION AND CONTROL
ELECTRODES FOR SPACECRAFT NICKEL-CADMIUM CELLS

JUNE 9, 1966 to JUNE 9, 1967

CONTRACT NO.: NAS 5-10241

Prepared By

GULTON INDUSTRIES, INC.
Alkaline Battery Division
212 Durham Ave.
Metuchen, N. J.

for

GODDARD SPACE FLIGHT CENTER
Greenbelt, Maryland

Prepared by: Approved by:

S. Lerner   H. N. Seiger
Research Chemist   Director of Research

CHARACTERIZATION OF RECOMBINATION AND CONTROL ELECTRODES
FOR SPACECRAFT NICKEL-CADMIUM CELLS

by

S. Lerner and H. N. Seiger

ABSTRACT

The objective of this program was to develop a sealed nickel-cadmium cell having a signal electrode, whose signal can be used for spacecraft charge control in near earth orbits. In such orbits, signal-electrode charge control is made difficult by the residual oxygen pressure present in the cell at the end of discharge. One way of overcoming this problem is by incorporating an oxygen-scavenging electrode in the cell.

In the first phase of this work, the Gulton Adhydrode and fuel cell materials from Leesona Moos and American Cyanamid were critically evaluated for use as scavenger electrodes. The material developed by American Cyanamid (AB6X) was found best for recombination purposes.

The second phase dealt with the signal electrode. The work in this phase was limited to improving the effectiveness of the Adhydrode as a signal electrode by determining the optimum location for it in the cell. Cells constructed with the Adhydrode in the end of the pack, center of the pack, and U-shaped (around the pack edge) were tested. The best signal-to-pressure response was exhibited by the Adhydrode in the center of the pack.

The third phase involved design, construction and testing of cells making use of the results of phases one and two. These tests showed: 1) The recombination rate of oxygen in cells with scavenger electrodes is greater than that in cells without scavenger electrodes; 2) consequently, the cell pressure (and the Adhydrode signal) decays sufficiently during a short discharge to allow for immediate recharge, and the apparent point of vigorous oxygen generation is delayed when charging; 3) cells containing the AB6X fuel cell material have a hydrogen scavenging ability; and 4) cycling at 60% depth of discharge in a near-earth orbit is a feasible mode of operation with signal-electrode charge control. However, degradation in cycle life is experienced at this depth of discharge.

TABLE OF CONTENTS

LIST OF TABLES

LIST OF FIGURES

LIST OF FIGURES

I.   INTRODUCTION

The determination of the end of charge of sealed nickel-cadmium cells may be detected with auxiliary electrodes. There are basically two kinds of auxiliary electrodes. One uses noble metals or silver as electrocatalysts and appears to follow a mechanism that is termed the perhydroxyl mechanism:

$$2\ O_2\ +\ 2H_2O\ +\ 4e^-\ \xrightarrow{\ i\ }\ 2\ O_2H^-\ +\ 2\ OH^-$$

$$2\ O_2H^-\ \xrightarrow{\ k\ }\ 2\ OH^-\ +\ O_2$$

$$O_2\ +\ H_2O\ +\ 4e^-\ \longrightarrow\ 4\ OH^-$$
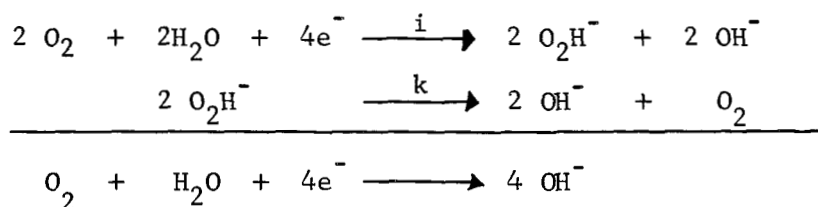
The other kind of auxiliary electrode does not rely on noble metals as electrocatalysts, and appears to follow a mechanism that is termed the adsorbed hydrogen electrode:

$$4H_2O\ +\ (M)e^-\ \xrightarrow{\ i\ }\ 4H(M)\ +\ 4OH^-$$

$$O_2\ +\ 4H(M)\ \xrightarrow{\ k\ }\ 2H_2O$$

$$O_2\ +\ H_2O\ +\ 4(M)e^-\ \longrightarrow\ 4\ OH^-$$
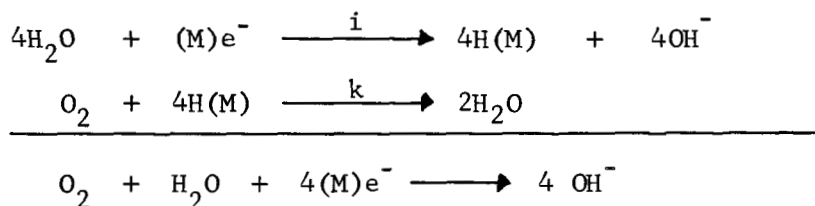
The term "adsorbed hydrogen electrode" has been condensed simply to Adhydrode ®. The differences between the two mechanisms are more than is shown by the two pertinent reactions. The most obvious difference lies in the fact that the oxygen consuming step is chemical in the Adhydrode scheme, and electrochemical in the perhydroxyl scheme. In the Adhydrode mode of charge control, the signal developed is almost linearly dependent on the partial pressure of oxygen in the cell.

Since the Adhydrode signal is dependent on oxygen pressure, it can be used in control systems designed to insure proper charging. The upper bound is exceeded if the rate and duration of charge causes the cell to explode due to pressure build up. The lower bound must be reached or the cell will not be fully charged. The number of ampere-hours of charge current must be greater than the number of ampere-hours of discharge current because the positive electrode is not 100% efficient in accepting charge.

The Adhydrode's basic property is its sensitivity to oxygen. The oxygen pressure in the cell is dependent, in turn, upon the cell itself and the cycle regime through which it passes. Under some cyclic conditions, such as short orbit periods of 90 minutes, the oxygen recombination rate is not great enough to allow the third electrode signal to diminish below the end of charge level. This condition, aggravated by the tendency of the Adhydrode signal to rise above the desired set point (a condition termed "overshoot"), prevents the cells from returning to a charge mode on the following cycle.

The rate at which oxygen is reduced, in a sealed cell, can be in-creased by including a scavenger electrode. It is the purpose of this work to develop cells having both signal electrodes and scavenger elec-trodes. A goal is to construct cells which are capable of cycling in near-earth orbits (90 minutes) using the Adhydrode as a charge control electrode. Thus, the improvements necessary are to increase the decay of the Adhydrode signal during a short (30 minute) discharge period and a more rapid recombination of oxygen.

The program was divided into three phases. The first involved evaluation of scavenger electrodes, including fuel cell as well as passive Adhydrode electrodes. The second part of the program was an evaluation of the third, or active, Adhydrode characteristics in regard to physical location. The final part of the program was devoted to test-ing cells containing the best features determined from the first two parts of the program.

II. PHASE I - SCAVENGER ELECTRODES

A scavenger electrode is an electrode which, when included in a cell, enhances the oxygen recombination rate. Two types of scavenger electrodes, excluding the sintered cadmium electrode, are available. These are: (1) the Gulton Adhydrode Ⓡ, and (2) the fuel cell electrode. Both types of material were investigated.

Scavenger Adhydrode electrodes of the following thicknesses and porosities were tested to determine their ability to recombine oxygen:

POROSITY (%)	THICKNESS (mils)
55	20
	55
70	20
	32
	55
85	20
	55

One type of fuel cell electrode from American Cyanamid and one type from Leesona Moos were also tested.

A. EXPERIMENTAL PROCEDURES & RESULTS

1. Synthesis of Adhydrode Scavenger Electrodes

In order to obtain Adhydrodes of the desired thicknesses and porosities for testing, several methods of synthesis were used. The starting materials were standard Adhydrode materials available from the Gulton Furnace Facility. The standard materials are 70% porous, and either 0.020 or 0.032 inches in thickness.

55% Porous Electrodes: The 0.020" electrodes were obtained by compressing a 70% porous 0.032" thick electrode with 30 tons of force. The 0.055" electrodes were obtained by building up a 70% porous 0.032" thick electrode to 0.065" thick by oversintering and then compressing with 30 tons of force.

70% Porous Electrodes: The 0.020 and 0.032" thicknesses were obtained from the Gulton Furnace Facility. The 0.055" thick electrodes were obtained by building up the 0.032" electrodes with additional catalyst material.

85% Porous Electrodes: The 0.020" electrodes were obtained by mixing the active catalyst material with a sawdust expander in a

ratio of 2/3 sawdust to 1/3 active material, placing the mixture on
a perforated nickel sheet, and then removing the expander by com-
bustion. The 0.055" electrodes were prepared by placing the active
catalyst directly on a 20 mesh, 7 mil nickel wire cloth.

2. Fuel Cell Electrodes

Two fuel cell electrode materials were also obtained.

AB6X Electrode: This material, obtained from American Cyanamid,
is 10 mils thick, has the active material attached to a metal wire
cloth, and has both sides available as active material.

Lesoona Moos Electrode: In this electrode, the active material
is held together by a Teflon coating on one side. Therefore, the
electrode has only one active surface. The active material is
pressed on an expanded metal screen and the entire electrode is
30 mils thick.

3. Testing of Scavenger Electrodes (Adhydrodes & Fuel Cells)

A sealed chamber was fabricated with a removable lucite top and
a pressure gauge. On the bottom of the cell, and insulated from
it, was a small flooded nickel-cadmium cell which was kept at
1.31 V by an external nickel-cadmium cell. The test material was
attached to the pressure gauge and was in contact with the electro-
lyte through a non-woven nylon (Pellon 2505K) wick (Figure 1. The
cell was then evacuated and pressurized to 45 psig (4 atm.) with
oxygen. A precision (1%) 0.5 ohm resistor was placed between the
test electrode and the flooded cell negative electrode, and the
voltage across the resistor was measured. This was repeated for
1 and 2 ohm precision resistors. The procedure was repeated again,
this time starting at 15 psig (1 atm.). From the voltage and re-
sistance, the current through the test electrode was calculated.
For each pressure, the current versus resistance was plotted and
extrapolated to R = 0, the condition for a passive catalyst.

The current density, i_o (R = 0), was plotted against pressure.
This graph, i_o versus P, is a measure of the recombination rate
for oxygen of the material under test. The results of the tests
are given in Table I and are graphically summarized in Figures 2
and 3. In the Table, the Adhydrode materials are referred to as
x/y where x is the thickness in mils and y is the percent porosity.

TABLE I

P Vs i_o FOR VARIOUS SCAVENGER ELECTRODES

P(PSIA)	LIMITING CURRENT, i_o, AS R ⟶ 0								
	20/55	20/70	20/85	32/70	55/55	55/70	55/85	Leesona	AB6X
60	1.40	2.24	1.86	2.08	1.91	1.98	2.72	3.94	20.8
45	1.20	2.02	1.66	1.80	1.62	1.81	2.40	3.42	20.3
30	1.02	1.80	1.31	1.68	1.44	1.50	1.90	2.83	19.6
15	0.88	1.51	1.04	1.35	1.20	1.20	1.59	2.60	18.9

i_o = milliamperes/sq. inch   x/y = thickness (mils)/porosity (%)

-4-

As shown in Figure 2, there is not very much difference in re-combination ability of the different Adhydrode materials tested. The best scavenger is the 55 mil thick-85% porous material, and the poorest is the 20 mil thick-55% porous material.

While the 55 mil-85% porous Adhydrode apparently has the best recombination properties, it was decided to use the 20 mil-70% porous Adhydrode for inclusion in test cells. There are several reasons for this choice; among them are: (1) there is not much dif-ference in properties and the 20 mil-70% porous electrode is readily available; (2) the highly porous electrodes do not adhere well to the substrate material and tend to flake and this may cause internal shorting in a cell; and (3) the thick plate is almost three times the thickness of either the positive or negative electrode, and its inclusion in a cell would require excessive compression to allow the electrode stack to fit in the cell case.

A comparison of the data shown in Figure 3 with that of Figure 2, indicates that the Leesona Moos electrode is about twice as good, and the AB6X electrode about ten times as good as the tested Adhydrodes. However, the Leesona Moos electrodes are active only on one side, while the American Cyanamid AB6X is active on both sides. An additional consideration is thickness. The AB6X material is 0.010" thick, which is half the thickness of the battery electrodes (0.020"), while the Leesona Moos electrode is 0.030" or one-and-one-half times as thick as a battery electrode.

As a check on the validity of the above described tests, sealed cells were constructed using the best Adhydrode material and both the American Cyanamid and Leesona Moos fuel cell electrodes.

To determine the effect of Adhydrode area on the rate of re-combination, cells were prepared having the negative-plate-to-Adhydrode-plate ratio of 10:1, 9:2, 8:3, and 7:4.

Design of Test Cells: Gulton positive, negative, and Adhydrodes were used. Plate dimensions were 2-3/4" x 2-3/4" x 0.020". Cells were constructed to 10 positive and 11 negative plates. Scavenger electrodes replaced negative plates. The separator material was Pellon 2505K, a non-woven nylon, and the electrolyte was 34% KOH.

Formation: Flooded cells were constructed and the electrodes formed using the following regime:

a. Charged at C/2 for 2 hours.
b. Charged at C/10 for 16 hours.
c. Discharged at C/5 for 5 hours.
d. Charged at C/4 for 7 hours.
e. Discharged at C/5 for 5 hours.
f. Charged at C/4 for 7 hours.
g. Discharged at C/5 to -1.0 V.

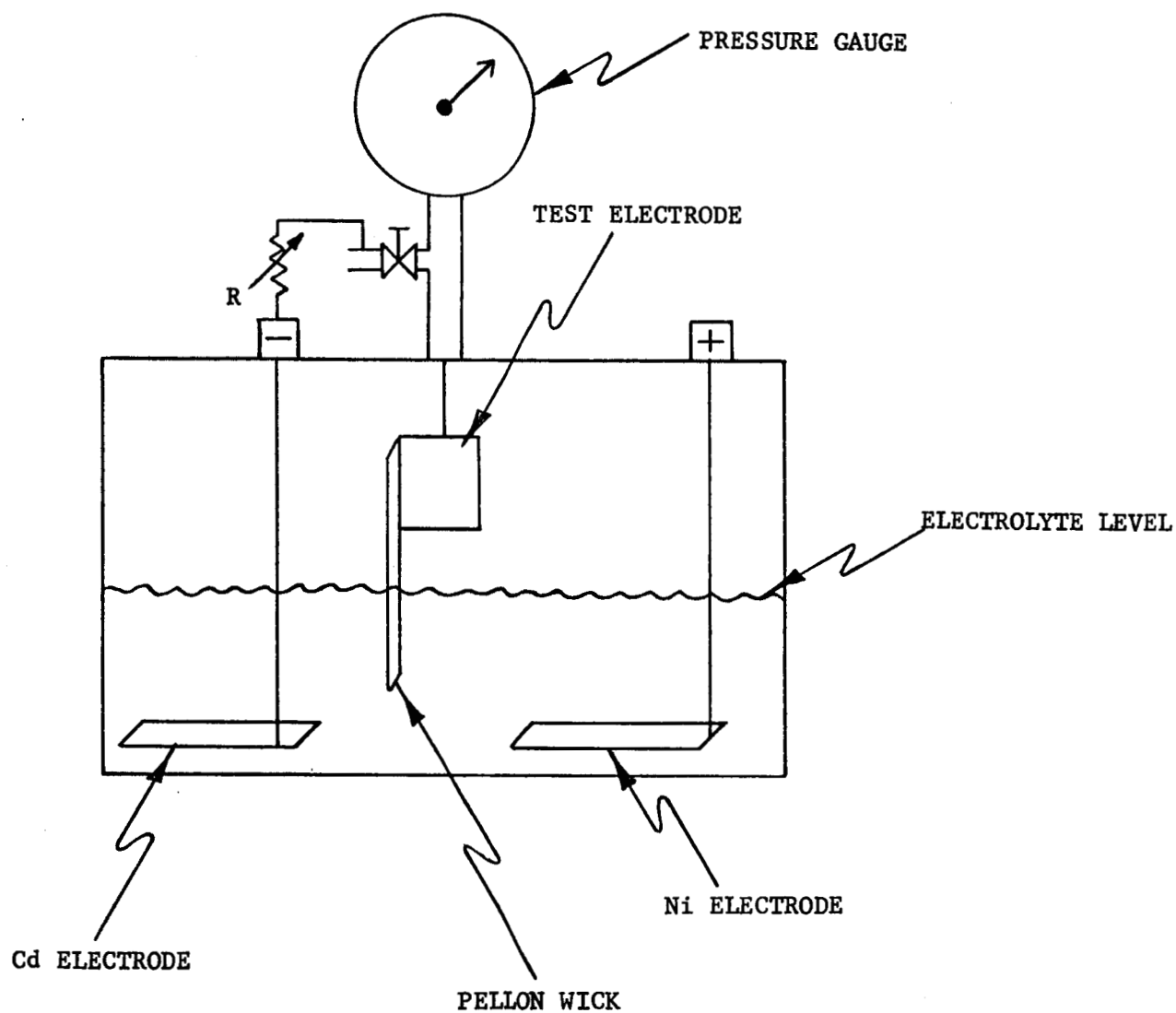Plates so formed were used for the construction of all sealed cells.

-5-

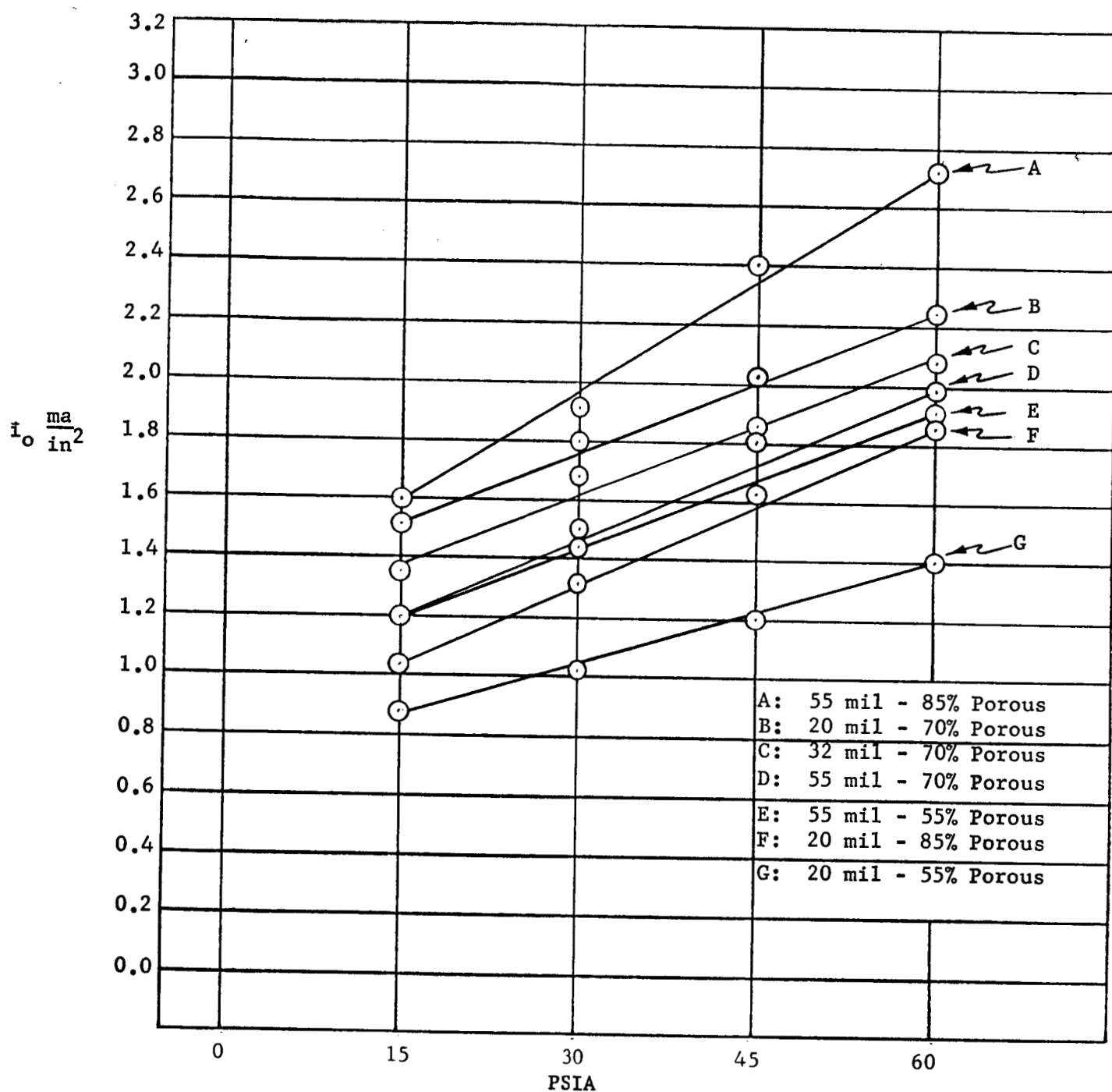FIGURE 1.   OXYGEN CONSUMING ELECTRODE TEST APPARATUS

5-1584

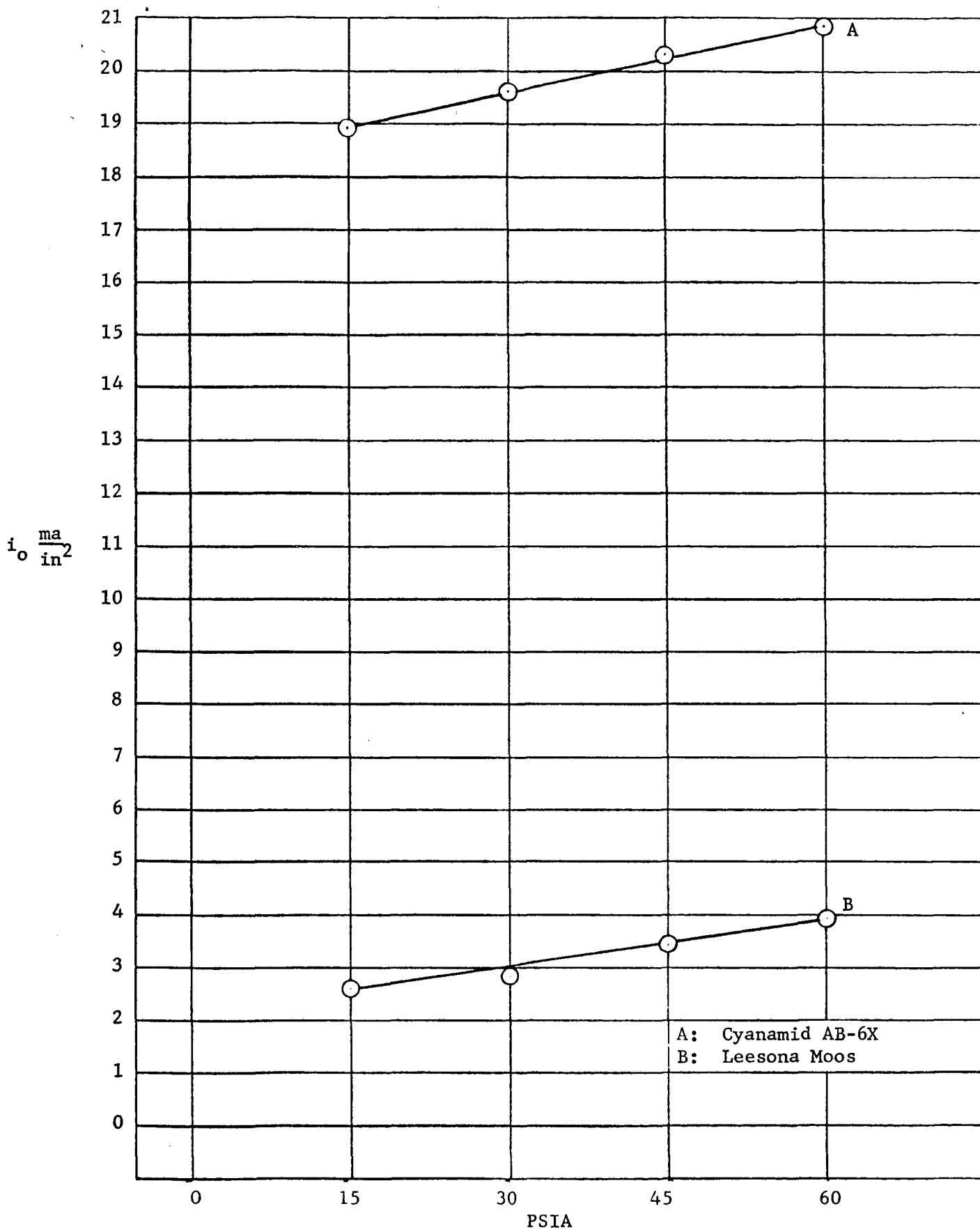FIGURE 2.   TEST OF PASSIVE ADHYDRODES

4-1585

FIGURE 3. TESTING OF PASSIVE FUEL CELL ELECTRODES

4-1586

4. Construction and Performance of Cells with Scavenger Electrodes

Eighteen test cells (number 1 through 18) were constructed using VO-12 size plates (70 mm x 70 mm), with six different configurations as shown in Table II. The cells were evacuated and the void volumes determined by a gas expansion method. This determination yielded a void volume of 102 cm^3.

The cells were again evacuated and charged to a 3 Ah input. The cells were then pressurized to 65 psia with oxygen, which was allowed to recombine (final pressure 3-5 psia). From knowledge of the void volume, it was calculated that the capacity of negative electrodes was reduced by 1.5 Ah. The cells were then discharged. The reduction of negative capacity insures that the positive exhausts first at the end of charge, thereby limiting the possibility of hydrogen evolution.

All cells were then placed on a 1.2 ampere charge to determine capacity on the subsequent discharge. These data for a 6.0 A discharge are also given in Table II.

Both the control cells and the cells containing four Adhydrodes in place of four negative electrodes were of low capacity, based on a 9.0 Ah theoretical capacity. However, the control cells showed minimal pressure (≤ 40 psia) which decayed on discharge, while the four Adhydrode cells generated high pressure (75-90 psia) which did not recombine on discharge, and was, by analysis, shown to be hydrogen. The presence of hydrogen indicated that the negative electrodes had become fully charged before the positive electrodes, which explaines the reduced cell capacity.

TABLE II

CONSTRUCTION & CAPACITIES OF SCAVENGER TEST CELLS

CELLS	NO. POSITIVES	NO. NEGATIVES	NO. & TYPE SCAVENGER	6 A DISCHARGE CAPACITIES
1	10	10	1 AB6X Fuel Cell	Leak
2	10	10	1 AB6X Fuel Cell	8.6
3	10	10	1 AB6X Fuel Cell	Leak
4	10	10	1 Leesona Moos Fuel Cell	Leak
5	10	10	1 Leesona Moos Fuel Cell	9.3
6	10	10	1 Leesona Moos Fuel Cell	9.2
7	10	10	1 Adhydrode	9.0
8	10	10	1 Adhydrode	8.4
9	10	10	1 Adhydrode	Leak
10	10	9	2 Adhydrodes	9.1
11	10	9	2 Adhydrodes	Leak
12	10	9	2 Adhydrodes	Leak
13	10	11	Control	Leak
14	10	11	Control	7.6
15	10	11	Control	7.6
16	10	7	4 Adhydrodes	Leak
17	10	7	4 Adhydrodes	7.6
18	10	7	4 Adhydrodes	Short

Twelve additional cells (Nos. 19-30) were built with four different configurations as shown in Table III. The cells were charged and the negative electrodes discharged 1.5 Ah by the addition of oxygen. The cells were discharged. The cells were then subjected to four charge-discharge cycles at 5 amperes to determine their capacity. The results of these capacity tests are shown in Table IV. Based on the capacity data, cells 22, 23, 24, and 26 were chosen for further testing, rated at 9.5 Ah capacity, and placed on a manual 55% depth of discharge cycle using a 90 minute orbit with a 20% overcharge. After 9 cycles, all the cells had run down to an end-of-discharge voltage of 1.0 volt or less.

In order to determine if the lost capacity could be regained, the cells were to be charged until the pressure reached 50 psig at 5 amperes and then discharged.

Cells 22 and 26 were discharged after reaching 50 psig and yielded 9.8 and 9.4 Ah capacity to 1.0 V, respectively. However, after 5 hours (25 Ah input), cells 23 and 24 had not reached the cutoff pressure. The cells were then discharged. This cycle was repeated twice more with the same result. A typical cycle is shown in Figure 4.

Cells 23 and 24 were placed on automatic cycle at a 55% depth of discharge with a 10% overcharge. The cycle consisted of 60 minutes of charge followed by 30 minutes of discharge. Both cells completed 113 cycles, with cell 23 operating at a pressure of between 1 and 10 psia and cell 24 operating between 40 and 50 psia. Cells 22 and 26 were not cycled due to excessive pressure buildup ($>$75 psia) on charge. At the end of charge, on the 114th cycle, cell 24 catastrophically failed at 50 psia; voltage measurements indicated that the cell had not shorted. A post mortem of the cell revealed that the separator had melted on the bottom edge of two of the plates at one end, possibly causing a temporary short circuit.

Cell 23 was placed back on cycle and completed 500 cycles before failure due to faulty terminal welds.

TABLE III

CONSTRUCTION OF CELLS WITH FUEL CELL SCAVENGER ELECTRODES

CELL NO.	NUMBER POSITIVE PLATES	NUMBER NEGATIVE PLATES	NO. & KIND SCAVENGER ELECTRODES
19-21	10	10	Control Cells
22 -24	10	11	1 AB6X
25-27	10	10	2 AB6X
28-30	10	10	1 Leesona Moos

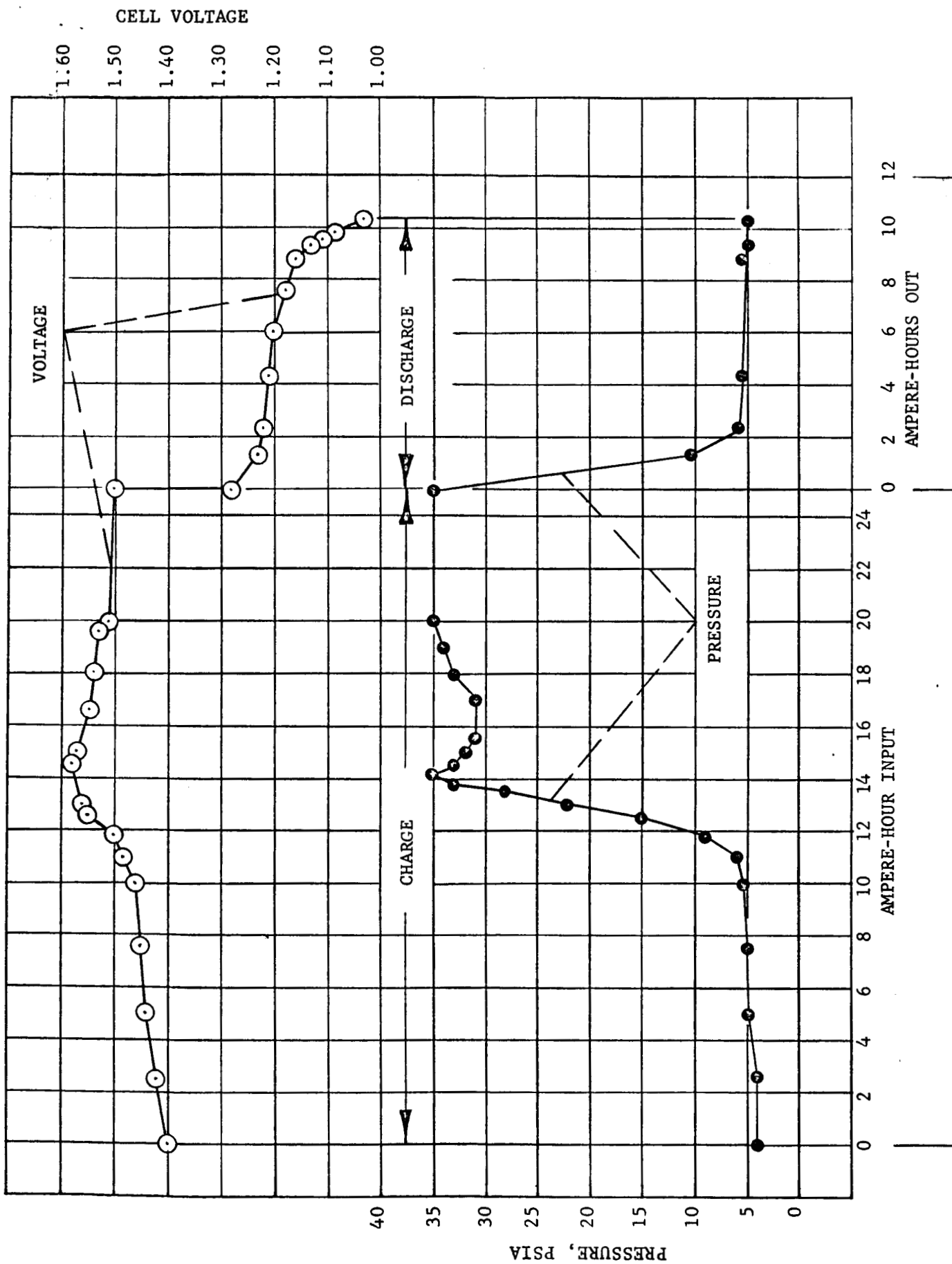Note: Cells 21, 25, and 27 were shorted and not tested.

FIGURE 4   TYPICAL CYCLE, CELL 23 OR 25, 5 AMPERE CHARGE & DISCHARGE

-11-

TABLE IV

CAPACITY DETERMINATIONS OF CELLS WITH FUEL CELL
SCAVENGER ELECTRODES

CYCLE	CONTROL CELL		1 AB6X CELL			2 AB6S	1 LEESONA MOOS		
	CELL 19	CELL 20	CELL 22	CELL 23	CELL 24	CELL 26	CELL 28	CELL 29	CELL 30
1	10.3	10.2	10.9	10.8	10.8	11.0	10.0	9.3	9.3
2	8.8	8.8	10.1	9.2	9.5	9.3	9.3	8.7	8.3
3	8.9	8.8	10.2	9.5	9.3	9.6	9.1	8.7	8.7
4	8.3	8.0	9.8	9.5	9.3	9.5	8.8	8.8	8.1
Avg. Last 3 cycles	8.7	8.5	10.0	9.4	9.4	9.5	9.1	8.8	8.4

With these factors in mind, namely, the hydrogen evolution of cells with Adhydrodes replacing negative electrodes, the thickness of the AB6X (10 mil) as compared to the Leesona Moos material (30 mil), and most significantly, the exceedingly rapid scavenging ability of the AB6X as compared to the Adhydrode or Leesona Moos material, it was decided that the AB6X material would be used as the scavenger electrode in the final design.

III. PHASE II - ACTIVE ADHYDRODES

The active Adhydrode is an electrode which, when connected through
a load resistor to the negative electrode, is used to monitor the end of
charge. This phase dealt with the improvement of the Adhydrode-signal-to-
pressure ratio by investigating the ratio as a function of the various
possible positions for the Adhydrode in the cell pack; i.e., "U" shaped,
in the center, and on one end of the pack.

A. EXPERIMENTAL PROCEDURES & RESULTS

1. Sensitivity As a Function of Position

Nine cells with active Adhydrodes were built. Three cells had
the Adhydrode in the "U" shape, three had the Adhydrode at one end
of the pack, and three had the Adhydrode in the middle of the pack.
The construction of these cells is shown in Table V. In all positions
the Adhydrode area was the same.

TABLE V

CONSTRUCTION OF CELLS WITH ACTIVE ADHYDRODE

CELL NO.	NUMBER POSITIVE PLATES	NUMBER NEGATIVE PLATES	NUMBER & POSITION OF ADHYDRODE
31-33	10	10	1 U-Shaped
34-36	10	10	1 End of Pack
37-39	10	10	1 Middle of Pack

NOTE: Cell 31 was shorted and not tested

Before testing, the cells were pressurized with enough oxygen to
reduce the capacity of the negative by 1.5 Ah. Three charge-discharge
cycles at 5 A were completed. During the charge, both the pressure
and Adhydrode signal (across a 1 ohm resistor) were monitored. A
typical Adhydrode signal and pressure curve for each of the three
Adhydrode positions is shown in Figures 5 to 7. Figure 8 is the
Adhydrode signal versus pressure curve for each of these configura-
tions. The trend shown by these figures is followed in the other
cycles, in that the Adhydrode place in the center of the pack showed
a consistently greater signal-to-pressure ratio than the Adhydrodes
placed in either of the other two positions.

A possible explanation for the experimental results is the avail-
ability of water to the Adhydrode. In the "U" position, water is
available only due to the wicking action of the separator. However,
when the Adhydrode is in the pack, water is available by direct con-
tact with that absorbed in the electrodes and separator. Also, the
Adhydrode in the center of the pack has both sides in contact, while
in the end position, only one side is in direct contact with the liquid
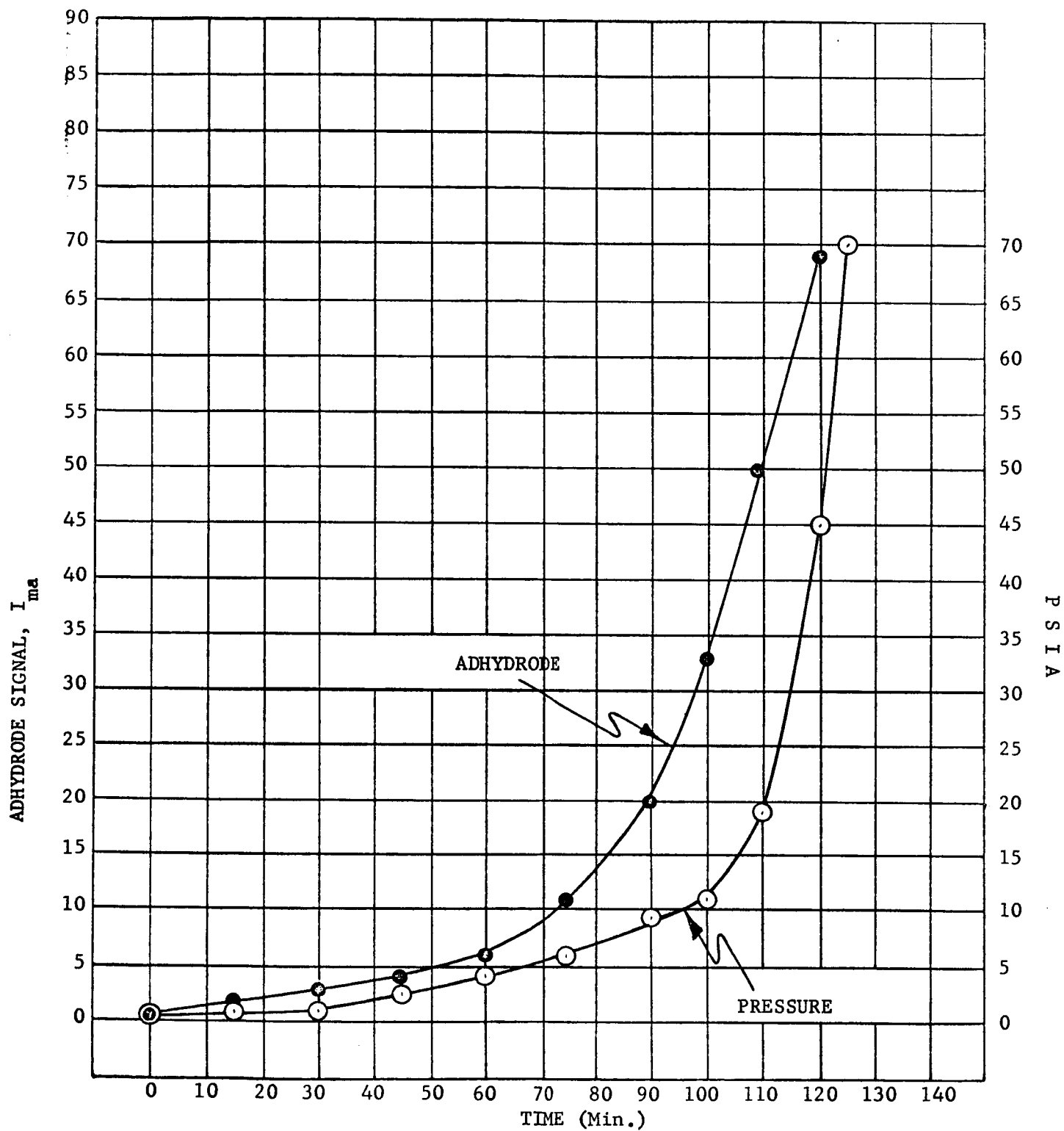phase.

-13-

FIGURE 5.   ADHYDRODE SIGNAL AS A FUNCTION OF POSITION
"U" SHAPED

4-1011
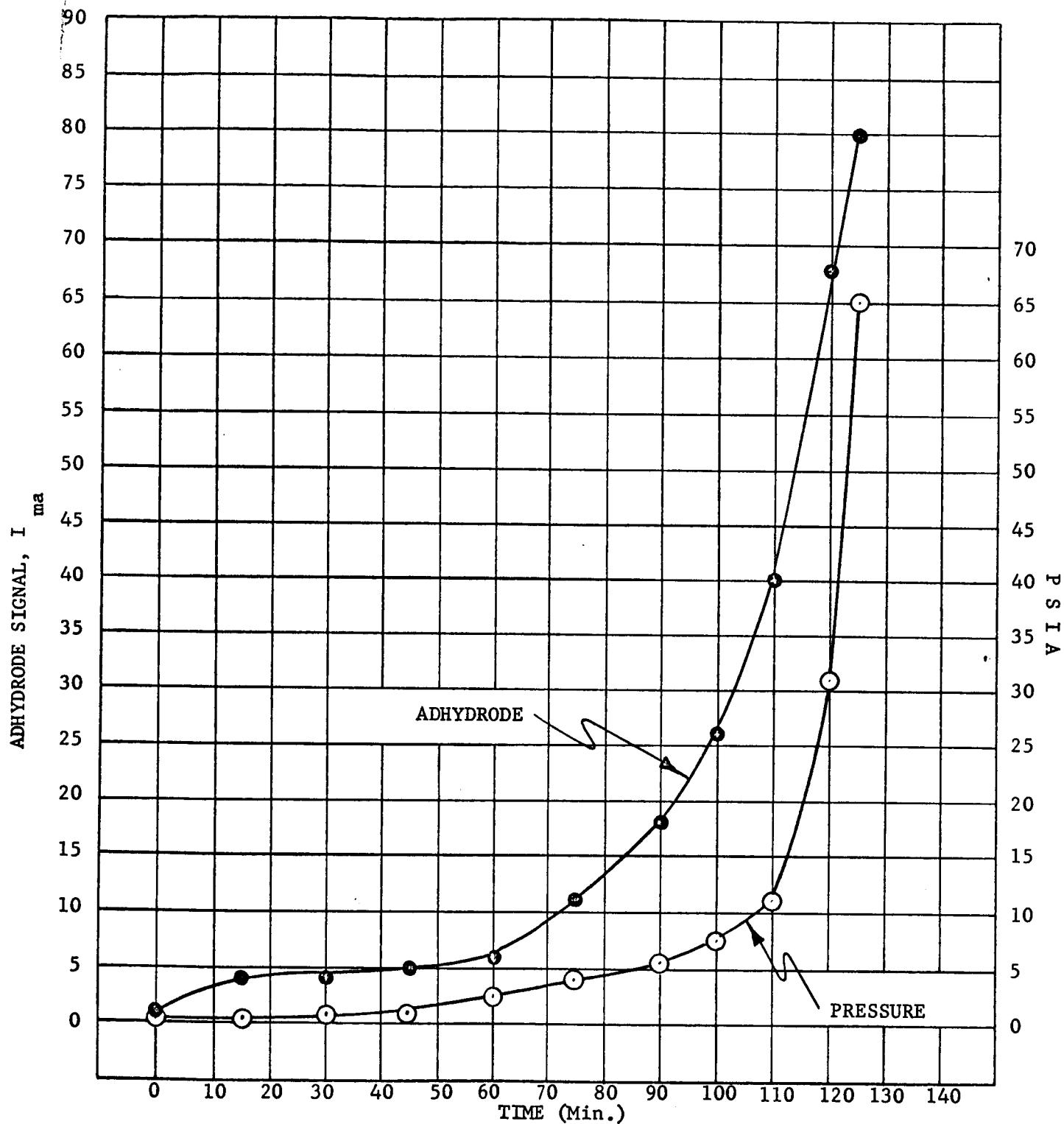
FIGURE 6.   ADHYDRODE SIGNAL AS A FUNCTION OF POSITION
END OF PACK

4-1012
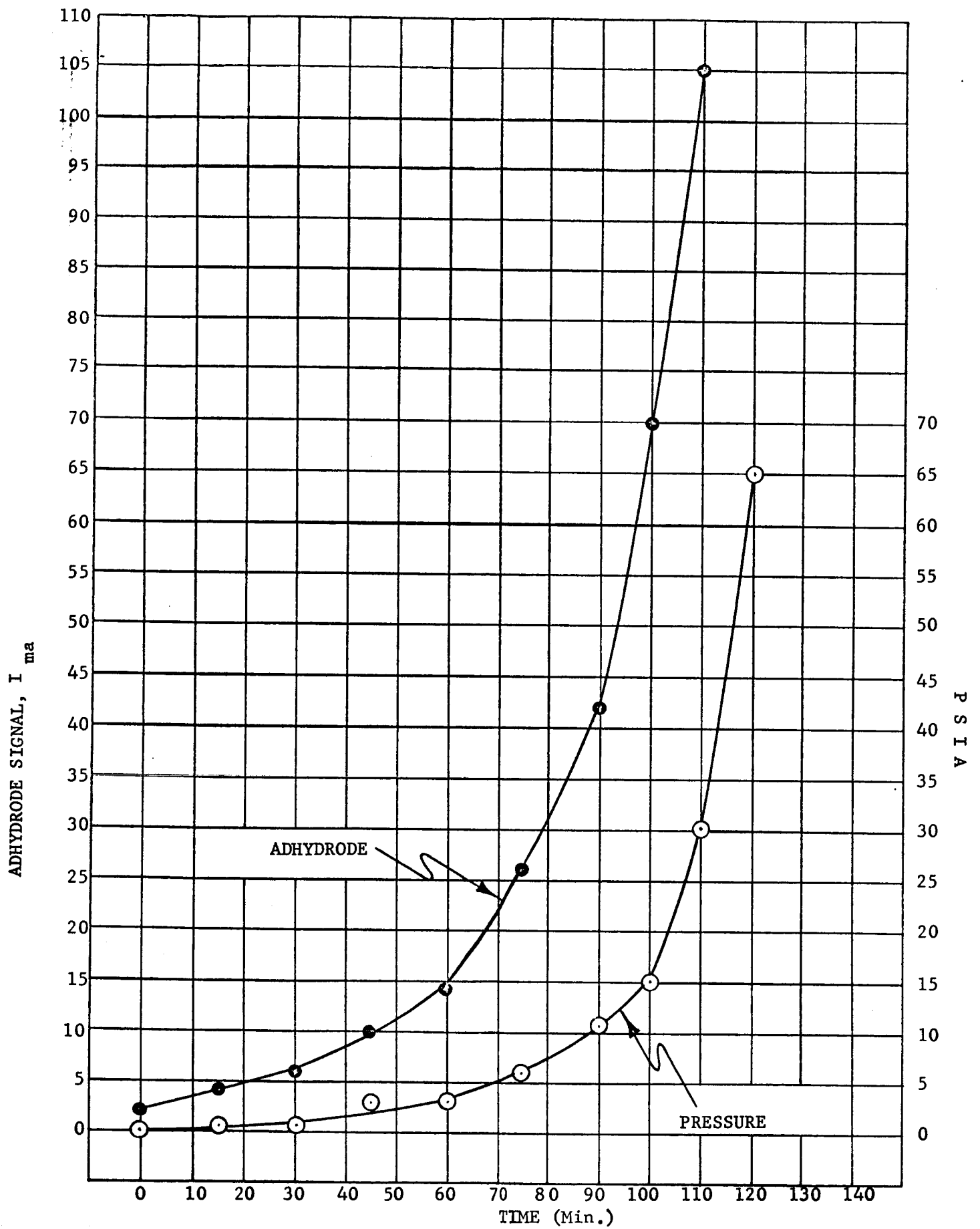
FIGURE 7.   ADHYDRODE SIGNAL AS A FUNCTION OF POSITION
MIDDLE OF PACK

4-1795
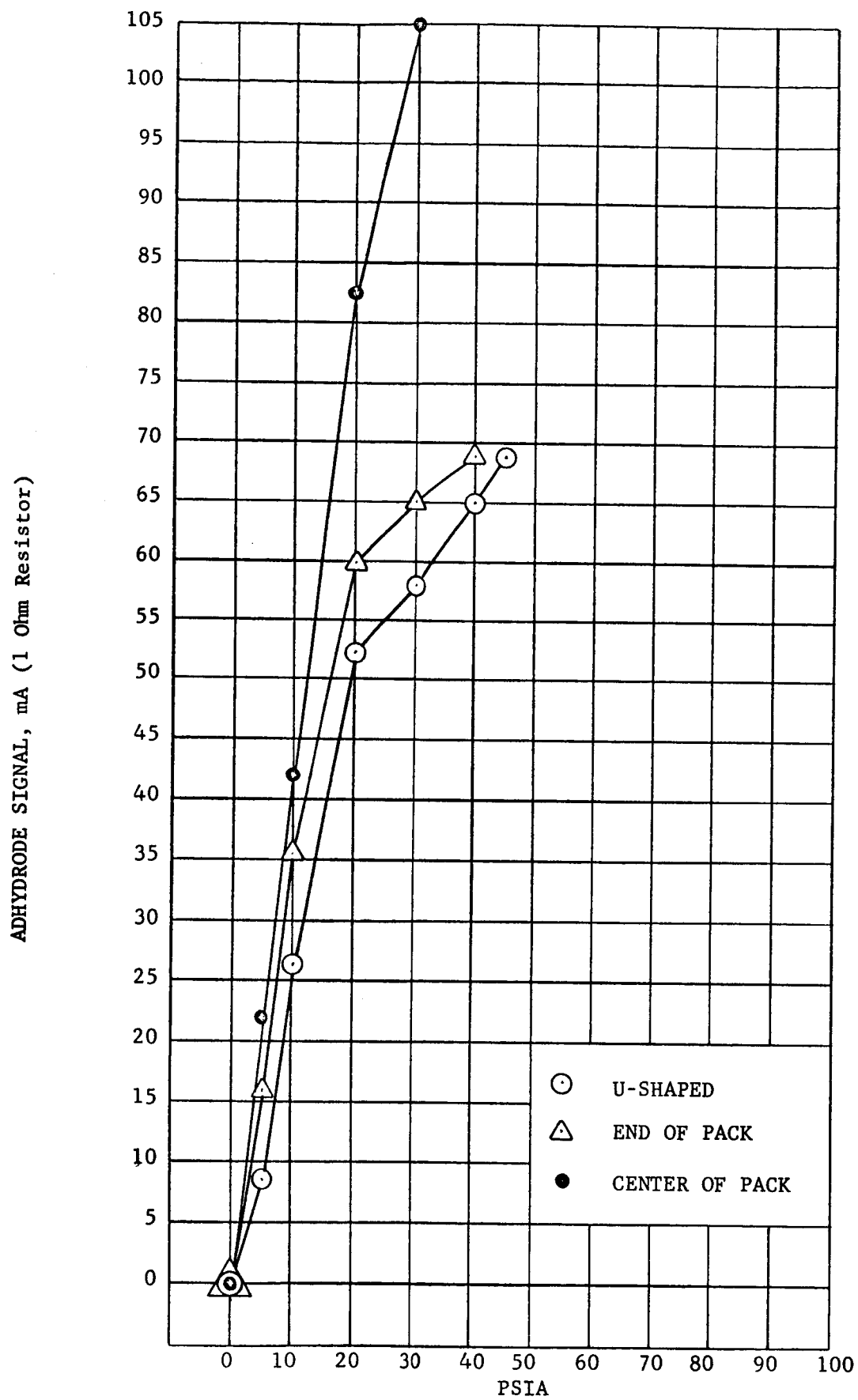
FIGURE 8   ADHYDRODE SIGNAL VERSUS PRESSURE

4-1783

2. Adhydrode Sensitivity as a Function of Load Resistor

The Adhydrode sensitivity is defined as the slope of the pressure versus signal curve for a specific load resistor. The load resistor is defined as the resistor placed in series between the Adhydrode and the negative electrode. Figures 9 and 10 are the Adhydrode sensitivity curves for 1/4, 1, 7, and 100 ohm resistors.

FIGURE 9   ADHYDRODE SENSITIVITY, 4 AMPERE CHARGE

FIGURE 10   ADHYDRODE SENSITIVITY, 4 AMPERE CHARGE

IV. PHASE III - CONSTRUCTION & TESTING OF CELLS WITH SCAVENGER ELECTRODES & ACTIVE ADHYDRODES

In this phase of the project, the best parameters from Phases I and II were mated into cells for final testing.

Four cells with scavenger electrodes and active Adhydrodes were constructed. Each cell contained 10 positives, 11 negatives, 1 AB6X fuel cell electrode shorted to the negative te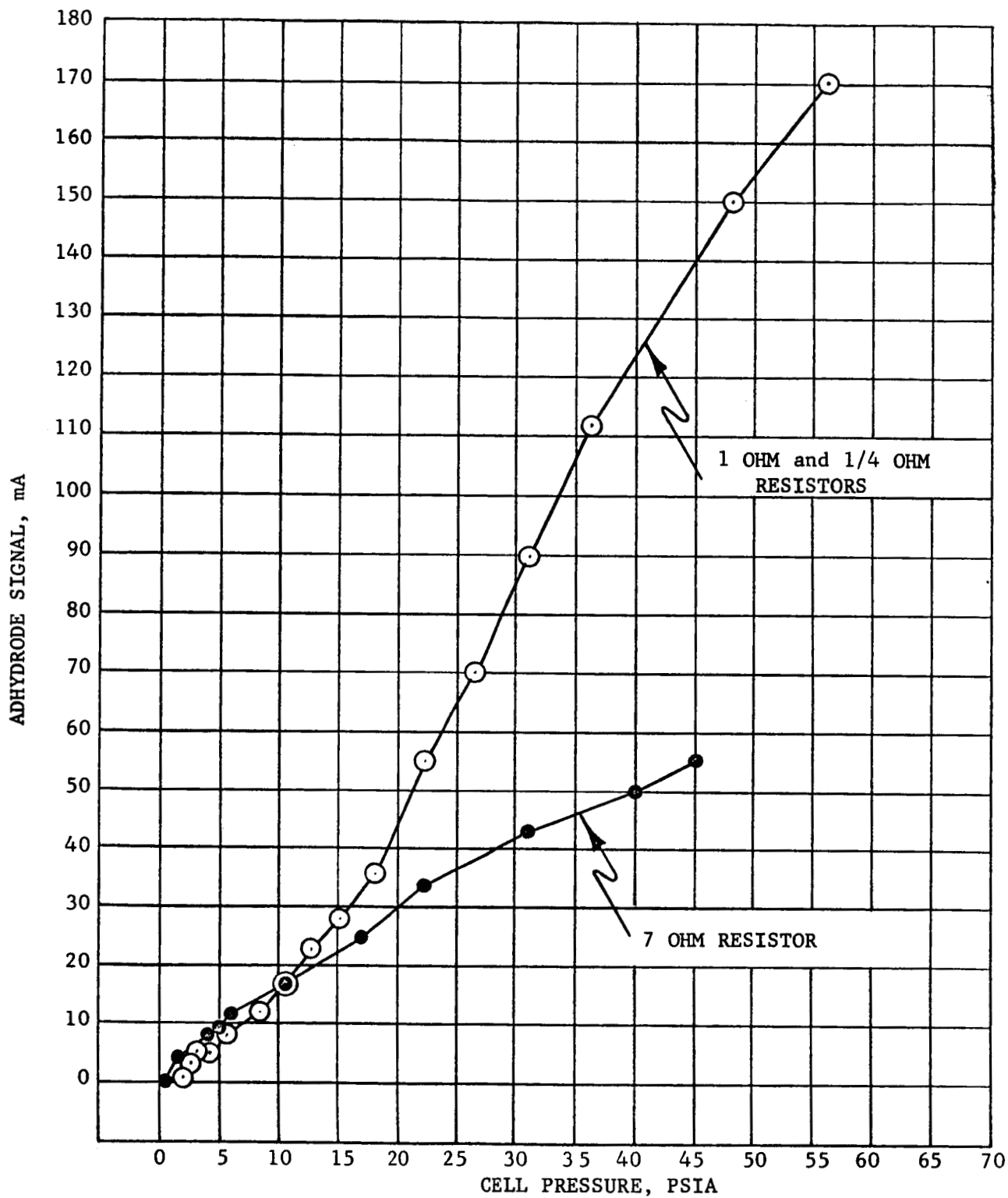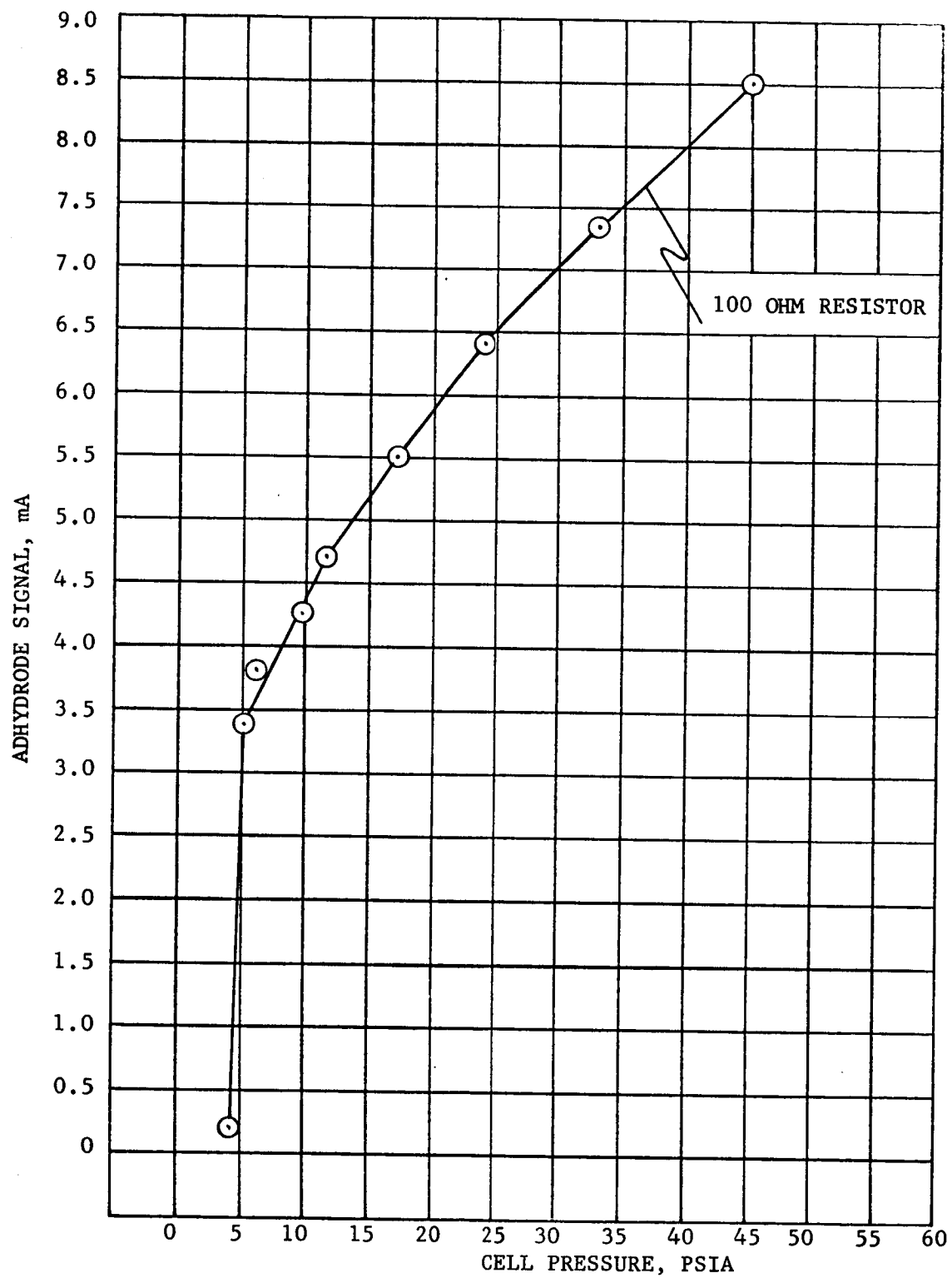rminal, and an active Adhydrode placed in the center of the pack and connected to a third terminal. The cells were numbered 40, 41, 42, and 43. After construction, the cells were pressurized with enough oxygen that the capacity of the negatives was reduced by 1.5 Ah. The capacities of the cells (1 ampere charge -- 5 ampere discharge) were as follows:

TABLE VI

CAPACITIES

CELL NO.	40	41	42	43	
CAPACITY Ah	8.3	8.5	6.4	8.0	

A. EXPERIMENTAL PROCEDURES & RESULTS

1. Automatic Cycling at Room Temperature

The four cells were manually cycled at a 50% depth of discharge on a 90 minute orbit (60 minute charge -- 30 minute discharge). Three of the cells (Nos. 41, 42, 43)* were placed on an automatic cycling routine which consisted of a 5.5 A charge for 60 minutes and a 9.5 A discharge for 30 minutes (60% DOD). This type of cycle allows for no open circuit stand between the end of charge and the beginning of discharge. However, even under this regime, two of the cells operated close to, or in, vacuum (P < 15 psia) and the third operated in the range of 15 to 40 psia. For these cycles, the Adhydrode signal was monitored but not used to terminate charge. This method of cycling continued for 476 cycles. Figure 11 is the Adhydrode and pressure curves for cell 42.

At the end of the above cycling, the three cells, rated at 8.0 Ah were manually cycled for four cycles using a 9.5 A discharge for 30 minutes (60%) and a 7.0 A charge. Both pressure and Adhydrode signal were monitored. A 1/4 ohm resistor was used as the load resistor. These cycles were used so that one cell could be chosen as the control cell (the one with the most reproducible Adhydrode signal) and the proper signal chosen as the trip point (the point at which charge is terminated). This cycling data indicated that cell 42 should be chosen as the control cell and the

---

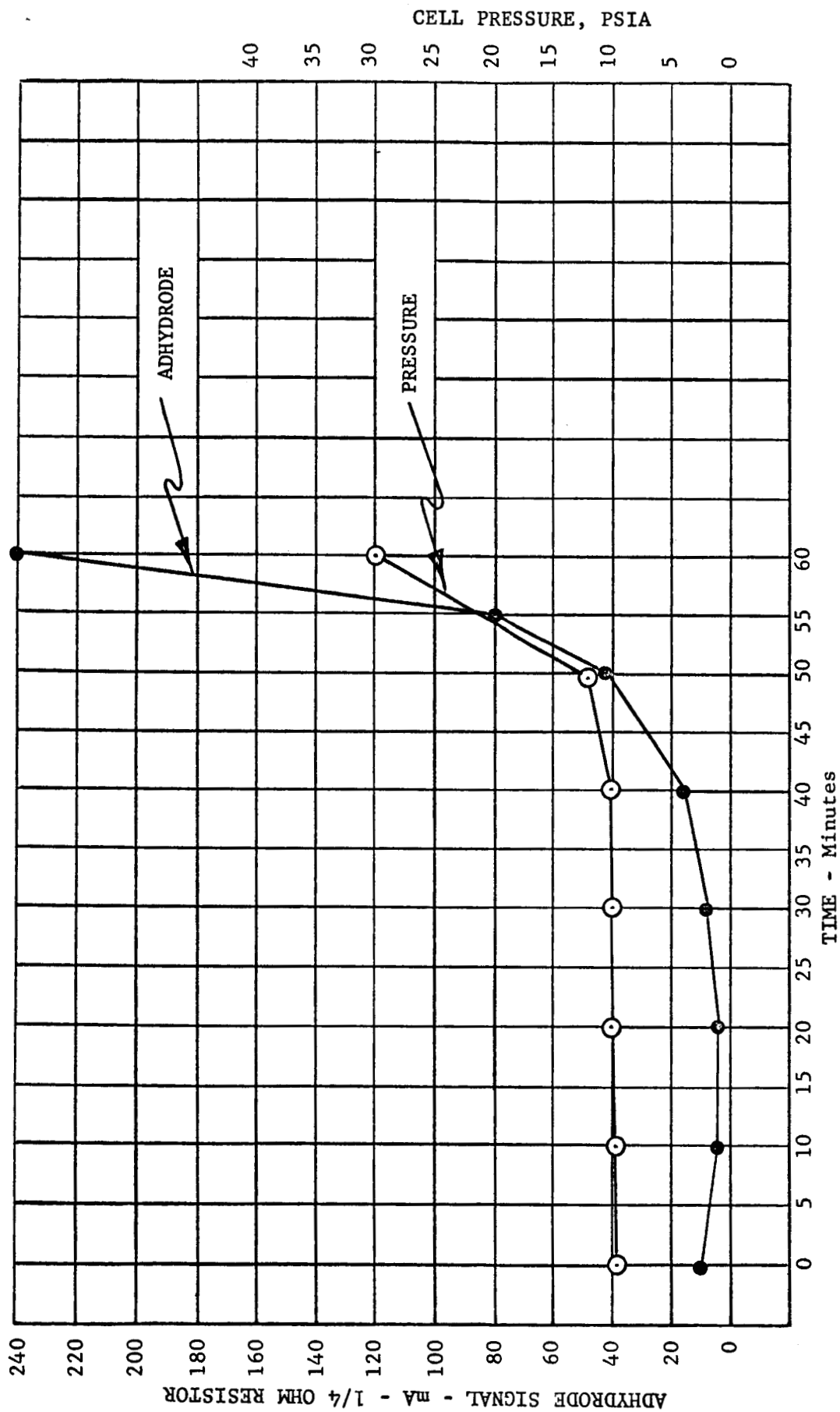* Cell 40 was not cycled due to the development of high pressure (> 65 psia) on charge.

FIGURE 11   ADHYDRODE SIGNAL - PRESSURE - AUTOMATIC CYCLING

CELL NO. 42, CYCLE 461, 60% DOD

5.5 A CHARGE - 10 A DISCHARGE

4-1192

-22-

trip point should be 200 mA (50 mV). This signal allows for a nominal 10% overcharge; i.e., the overcharge may vary slightly from one cycle to the next.

The cells were then placed on an instrument which allowed the cells to be charged for 60 minutes or to a preset Adhydrode signal, and discharged for 30 minutes. If the Adhydrode signal point is reached before the end of 60 minutes, the cells are then automatically placed on open circuit for the remainder of the 60 minutes, and then go on the discharge portion of the cycle. The cycle counter was reset to zero for cycling under Adhydrode control. The cycle was a 30 minute discharge at 9.5 A and a 7.0 A charge to the Adhydrode cutoff. Figure 12 is the Adhydrode and pressure curve for cycle 97 for the control cell (no. 42). After the 144th cycle, the end of discharge voltages began to fall below 1.0 V. This was due to a slight increase in the Adhydrode sensitivity, causing the cells to be removed from charge prematurely. In the cycle used, a 7.0 A input for 41 minutes corresponded to the output on discharge. Therefore, if the cells were removed from charge at 41, or less, minutes the cells would eventually run down. To compensate for this, the resistor was changed to 1/8 ohm and the trip point reset to 360 mA (45 mV). This again allowed for a nominal 10% overcharge. The resistor had to be changed since the instrument had a maximum full scale deflection of 50 mV.

Figure 13 is the Adhydrode signal and pressure for cycle 305. On the 326th cycle, the Adhydrode on the controlling cell ceased to function in a stable manner, and the cells began to receive a full 60 minutes of charge which corresponds to a 32% overcharge. However, even with this overcharge, the end of charge cell pressures remained below 40 psia, again indicating the utility of the scavenger electrode.

In order to determine the cause of the erratic Adhydrode behavior, the cell atmosphere in the control cell was analyzed after the end of charge of the 367th cycle and found to contain 95% hydrogen. Control and experimental cells both exhibited the presence of hydrogen. However, the presence of hydrogen in the cells and the low end-of-charge pressure (12 psia), along with the fact that during discharge the cell returns to vacuum, illustrates the advantage of using a fuel cell electrode as a scavenger, since the buildup of extreme pressures is prevented regardless of the composition of the internal cell atmosphere. After the gas sample analysis, the cells were discharged to 1.0 V and reconditioned. The reconditioning cycle consisted of a C/10 (800 mA) charge, a 3 ampere discharge to 1.0 V, a C rate charge, and a 3 ampere discharge to 1.0 V.

Since prior to cycling, cell 42 had a capacity somewhat lower than the other cells, it is probable that part of the difficulties which arose during cycling were due to the severe loss in capacity of the control cell as shown in Table VII.

TABLE VII

CAPACITIES OF CELLS 41, 42, and 43 AFTER CYCLING

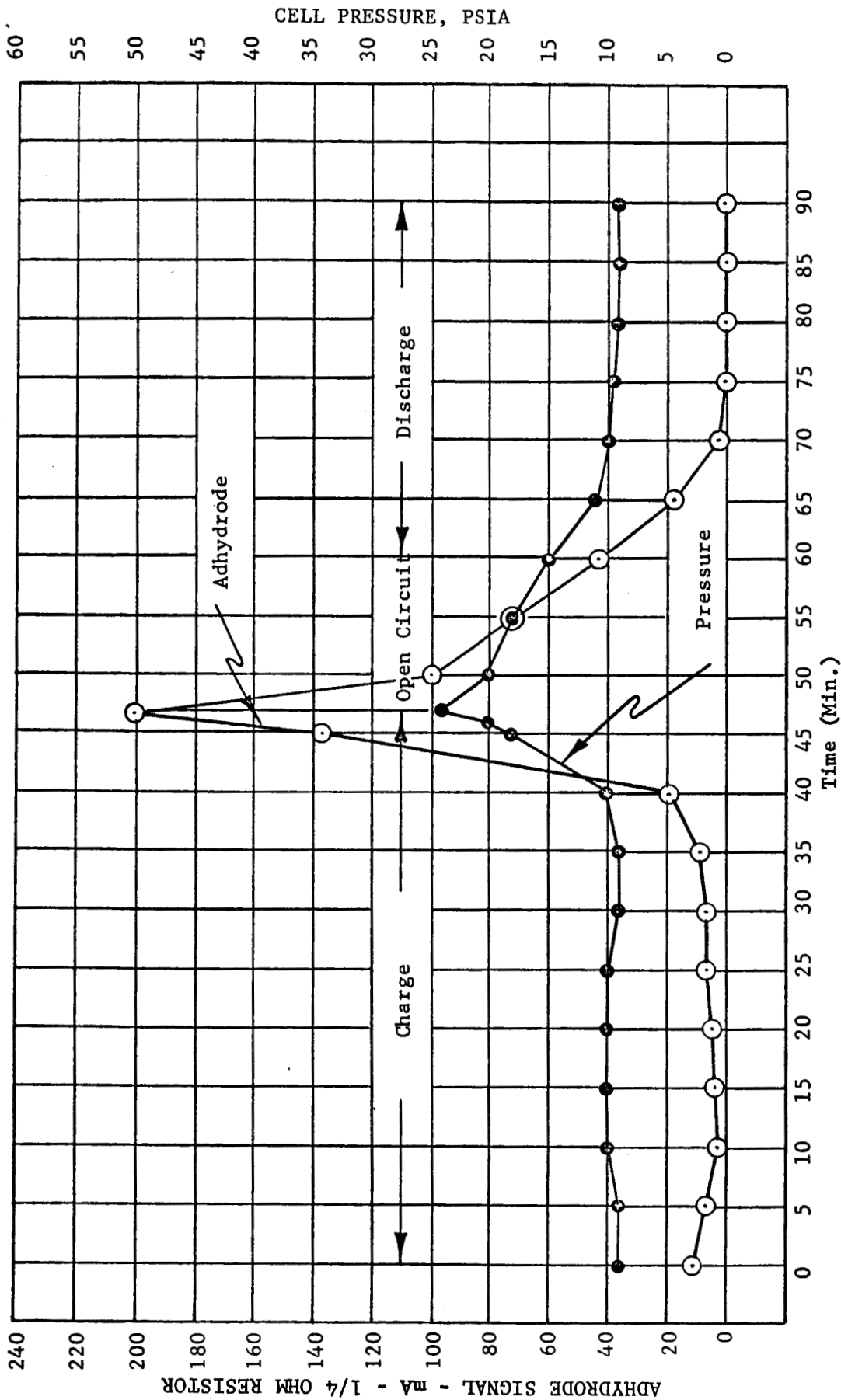| CELL NO.	41	42	43
CAPACITY (Ah)	7.8	5.1	7.7

Figure 12- Cell 42 60% DOD Cycle 97, Adhydrode Control
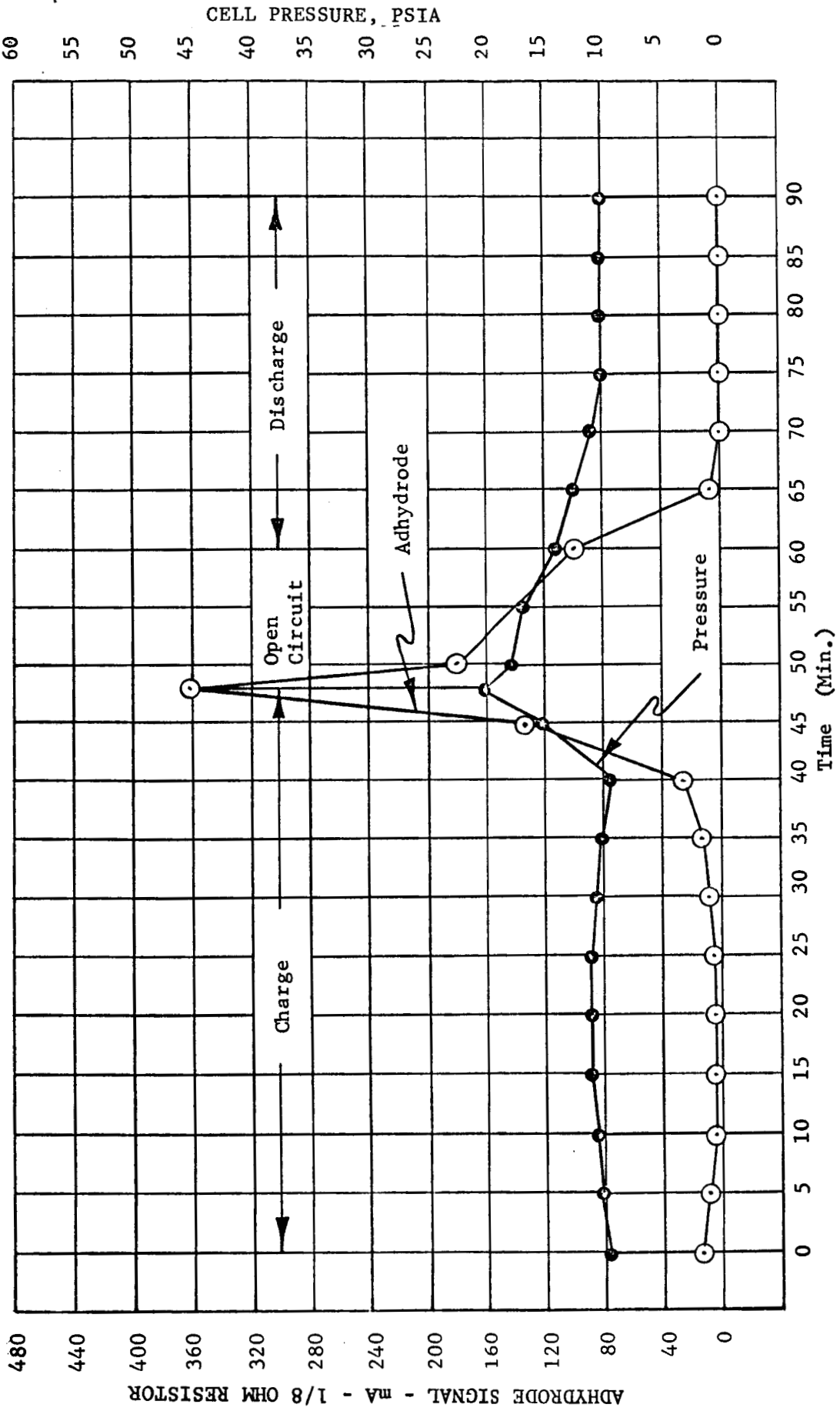7A Charge - 9.5A Discharge

Figure 13 - Cell 42 60% DOD Cycle 305, Adhydrode Control
7A Charge - 9.5A Discharge

4-1213

After the reconditioning cycle, two of the cells (nos. 41 and 43) were placed <u>back</u> on cycle with cell number 43 controlling. Figures 14, 15, and 16 are, respectively, cycles 61, 285, and 398. The cycle counter was reset to zero again.

At the end of charge of the 676th cycle under Adhydrode control, the cells were placed on open circuit for three days due to a power shutdown. When the cells were placed on cycle again (discharge portion), cell 41 went into reverse immediately. The cell was removed from cycle and a subsequent charge and discharge indicated a shorted cell.

Cell 43 was continued on cycle with the trip point reset to 280 mA (35 mV). Figure 17 is the 789th cycle. During charge on the 794th cycle, the cell voltage dropped to 0.0 V and remained there through the succeeding charge and discharge cycles, indicating that the cell had failed by shorting.

At the end of cycle life, cells 41 and 43 had, respectively, accumulated 1519 and 1637 cycles at 60% depth of discharge. While it is realized that an average cycle life of 1600 cycles is short compared to the usual cycle life of a nickel-cadmium cell, it must also be realized that the cycling conditions were much more stringent than usually applied, and that even at this severe depth of discharge, the internal cell pressure remained low, independent of cell atmosphere, and the recombination rate remained rapid.

The results of the cycle testing at 60% depth of discharge, at room temperature, indicate the utility of cells containing both an Adhydrode as a charge control electrode, and a fourth electrode as a gas scavenger electrode. In these cells, the Adhydrode signal which tracks the pressure closely, is strong at the end of charge, exhibits no overshoot of the trip point (i.e., the continued use of the Adhydrode signal above the trip point after the cells have been removed from charge), and decays rapidly on open circuit on discharge. The incorporation of a fuel cell scavenger electrode allows the cell to operate at low pressures independent of the composition of cell atmosphere and exhibits a rapid recombination rate.

2. Temperature Testing

Nine cells, numbered 46 to 54 were fabricated. These cells contained 13 positive electrodes, 14 negative electrodes, the Adhydrode in the center of the pack, and the fuel cell electrode on one end. The extra positive and negatives were added in order to increase the capacity of the cells.

a. Low Temperature

For these tests, the cells were operated at their actual capacity, 14 Ah for the control cells, and 9 Ah for the experimental cells.

FIGURE 14   ADHYDRODE SIGNAL AND PRESSURE, CELL 43, CYCLE 61, 60% DOD, ADHYDRODE CONTROL
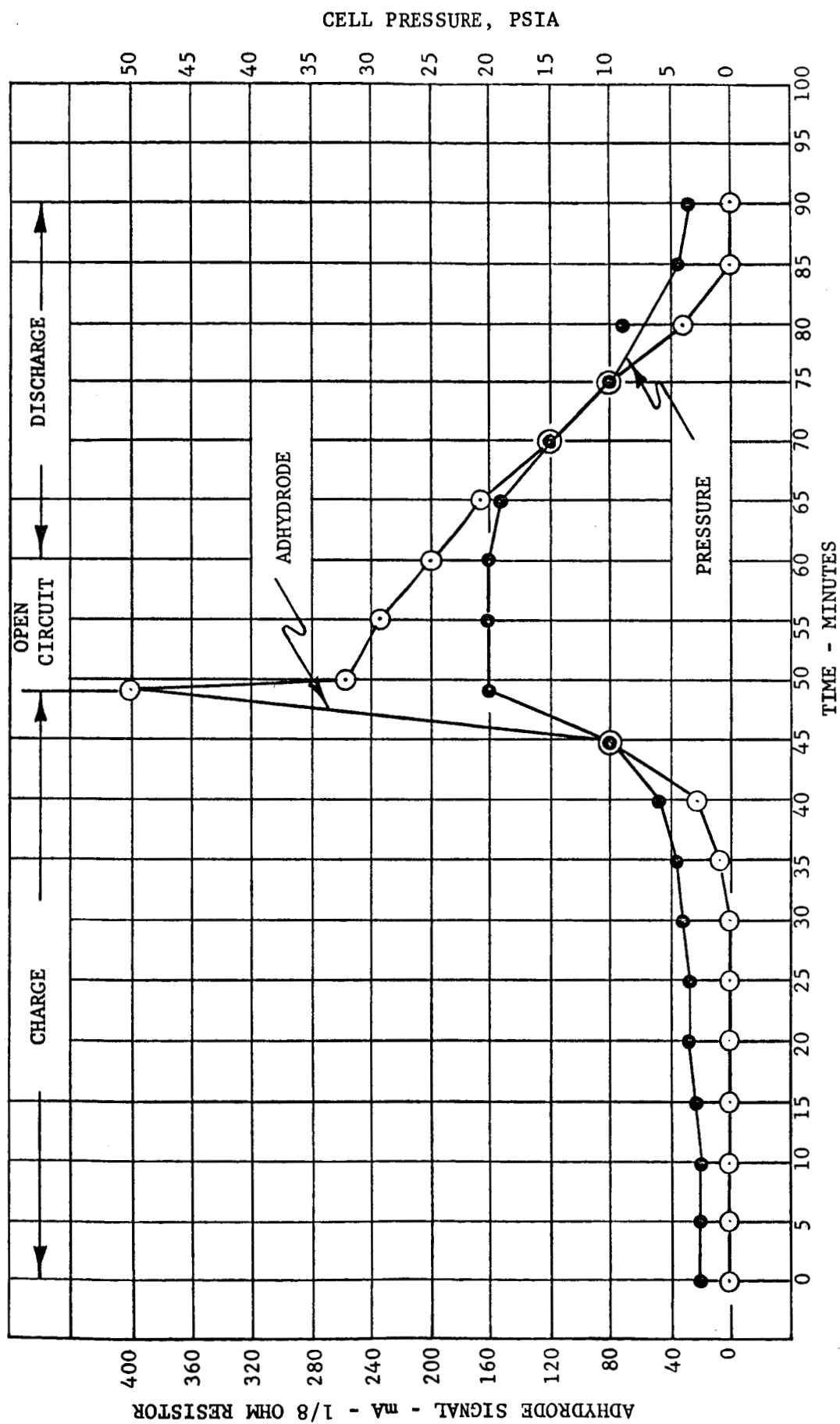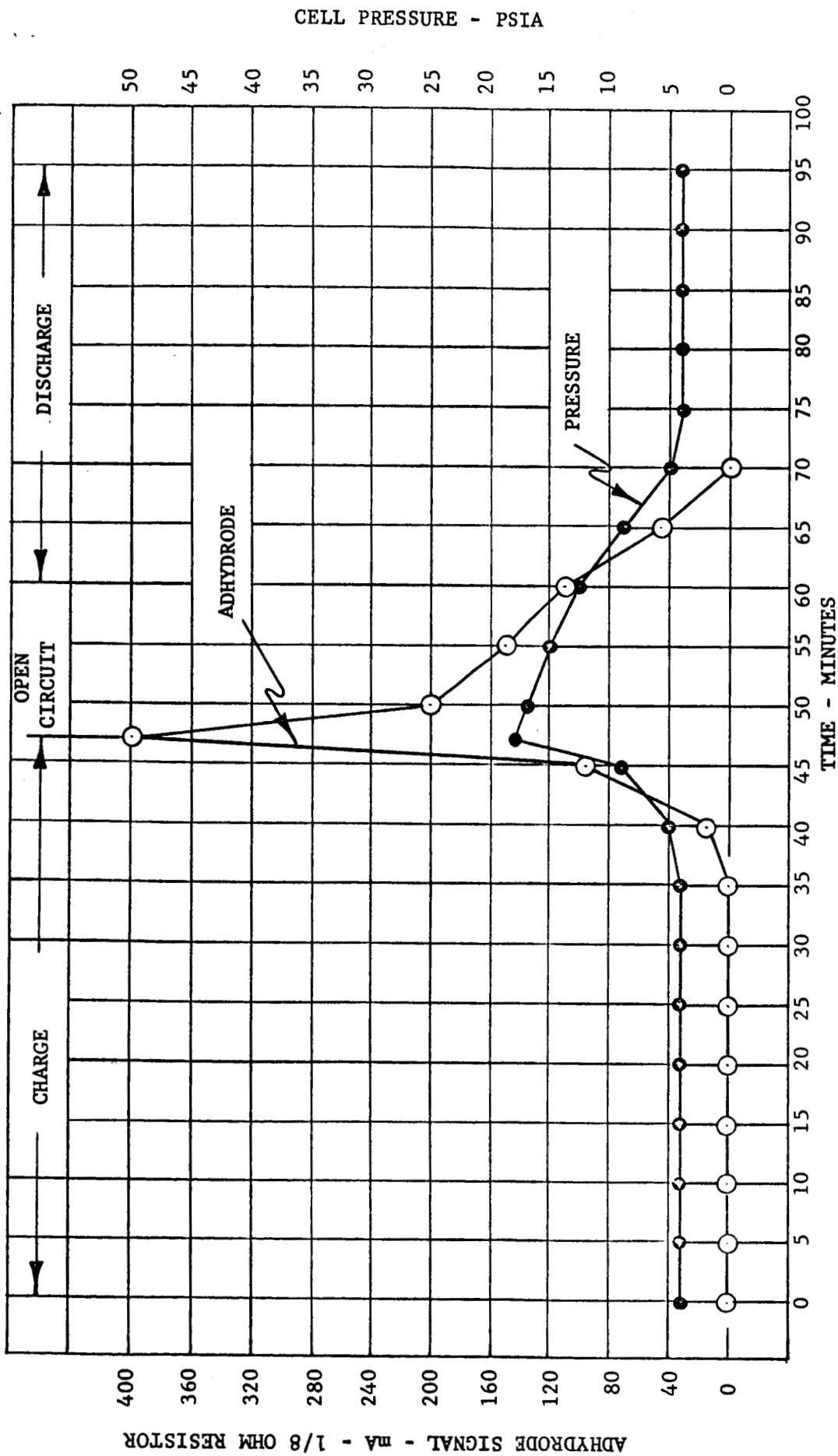7A CHARGE - 9.5A DISCHARGE

4-1503

-27-

FIGURE 15   ADHYDRODE SIGNAL AND PRESSURE - CELL 43, CYCLE 285, 60% DOD, ADHYDRODE CONTROL
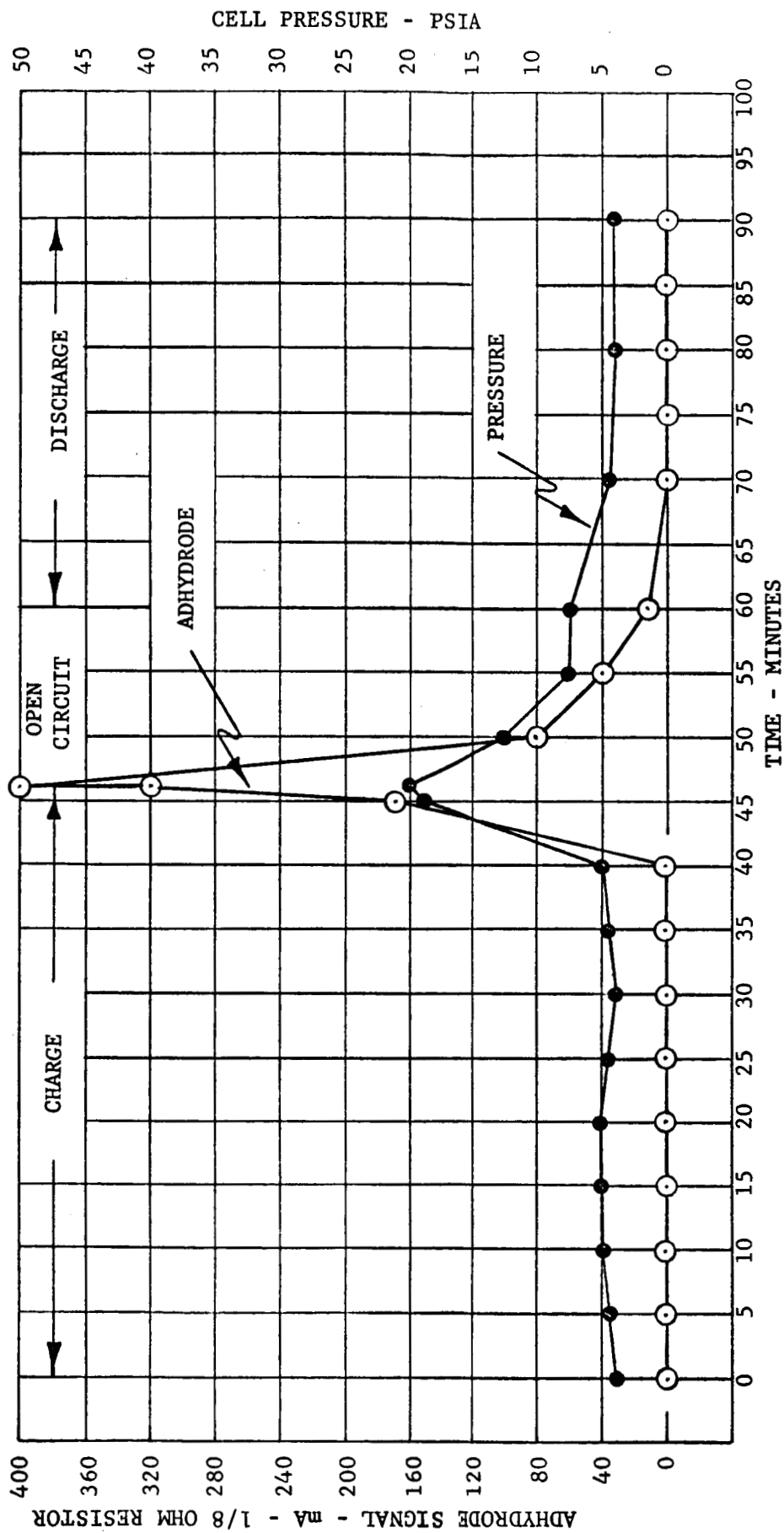7A CHARGE - 9.5A DISCHARGE

FIGURE 16   ADHYDRODE SIGNAL & PRESSURE, CELL 43, CYCLE 398, 60% DOD, ADHYDRODE CONTROL
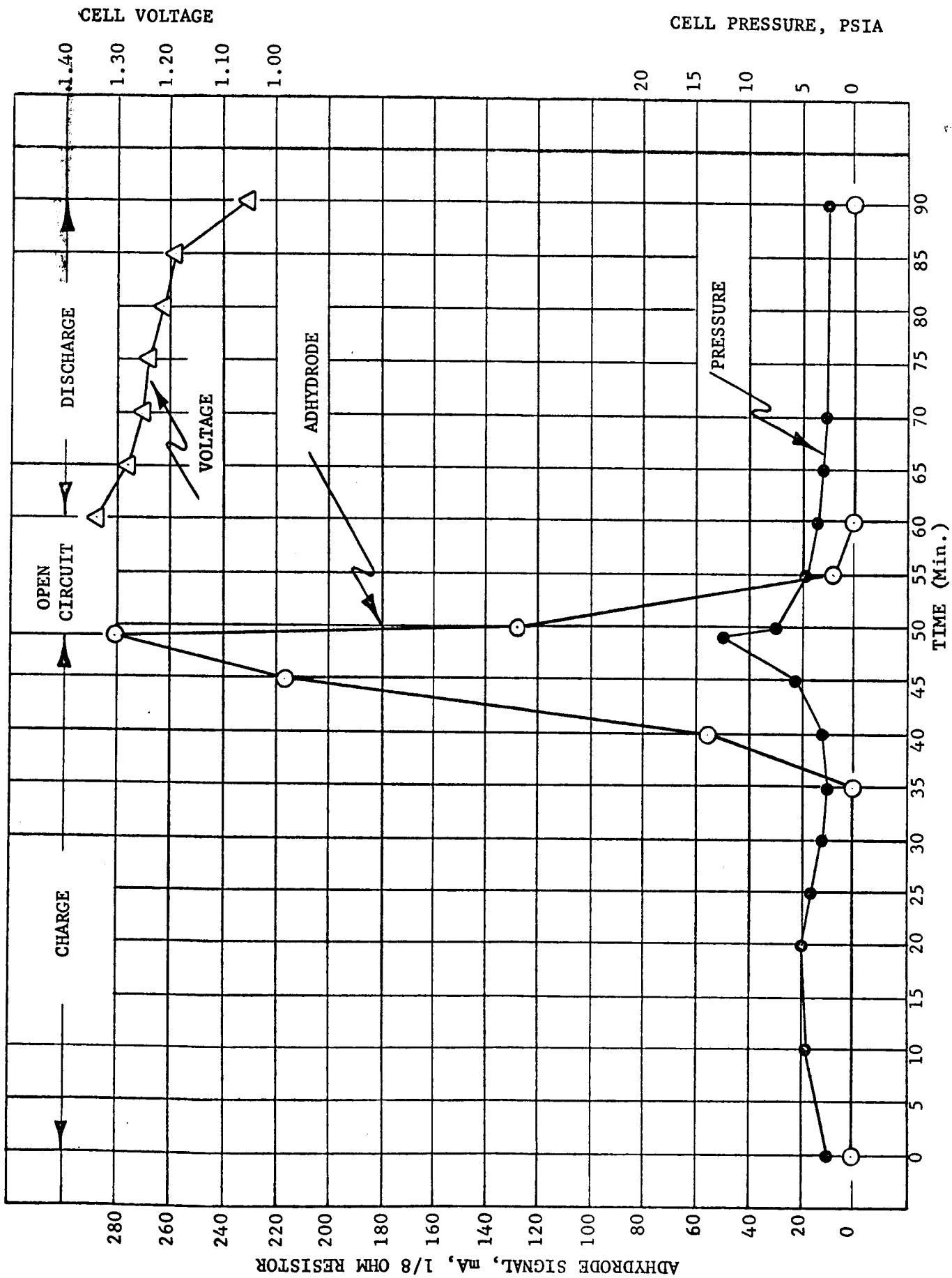
7A CHARGE - 9.5A DISCHARGE

FIGURE 17   CYCLE 789, 60% DOD, ADHYDRODE CONTROL, CELL 43
7 A Charge, 9.5 A Discharge

4-1556

Three of the control (VO-12HSAD standard 12 Ah Adhydrode) cells and three experimental cells were cycled for one week at both -20°C (-4°F) and 0°C (32°F) at a 50% depth of discharge on a 90 minute orbit. Sixty-five cycles were completed at -20°C, and 61 at 0°C. One complete cycle a day was monitored. Figures 18 through 21 are, respectively, the 3rd and last cycle for an experimental and control cell at -20°C. Figures 22 through 25 are similar curves at 0°C.

It should be noted that on the last cycle for the experimental cell at 0°C, the pressure begins to increase at the initiation of charge. The reason for this was not investigated and no explanation is offered. However, this pressure rise is slight (10 psia), and apparently has no effect upon the pertinent cell characteristic, i.e., pressure and Adhydrode signal decay. The experimental cells had a stronger Adhydrode signal than the control cells. This signal, even at these low temperatures, rose rapidly upon charge and decayed rapidly upon discharge. On the other hand, the Adhydrode signal from the control cells exhibited overshoot.

On the last cycle at each temperature, the cells were discharged to 1.0 V and there capacities were determined. These data are shown in Figures 26 and 27. It is evident that the experimental cells containing the fuel cell electrode have a greater resistance to capacity loss on low temperature cycling than the control cells. It should be noted that, at low temperatures, the capacity of nickel-cadmium cells generally increases. However, the magnitude of this increase should be the same for both sets (control and experimental).

b. High Temperature

Three VO-12HSAD control cells and three experimental cells containing fuel cell scavenger electrodes were placed in a chamber at 40°C (104°F) in the discharged state. The cells were allowed to stand for 48 hours and were then charged at 5 amperes. During the initial charge, the control cells developed exceedingly high pressures (greater than 150 psig). Analysis indicated that the gas was > 97% hydrogen. These cells, along with one experimental cell were removed from the oven and not tested further.

The remaining two experimental cells were placed on cycle at 50% depth of discharge. Both cells went into reverse on the first cycle. The two cells (discharged) were then allowed to equilibrate at 35°C (95°F). Eighteen cycles were completed before one cell went into reverse and the other cell's end-of-discharge voltage fell below 1.0 V (Figure 28). It is not known why the cells with fuel cell scavengers would not cycle at deep depths of discharge at 35° or 40°C.

To determine if the exposure to high temperatures had adversely affected the cells, the cells were placed on cycle at 50% depth of discharge for one week at room temperature. No problems were encountered during the room temperature cycling.

Figure 18- Cycle 3 Exp. Cell 50% DOD -20°C (-4°F)
9 A Discharge, 5 A Charge

Figure 19- Cycle 3 Control Cell 50% DOD -20°C (-4°F)
14 A Discharge, 7.7 A Charge

4-1215

-33-

4-1216

Figure 20 Cycle 65 Exp. Cell 50% DOD -20°C (-4°F)
9 A Discharge, 5 A Charge

-34-
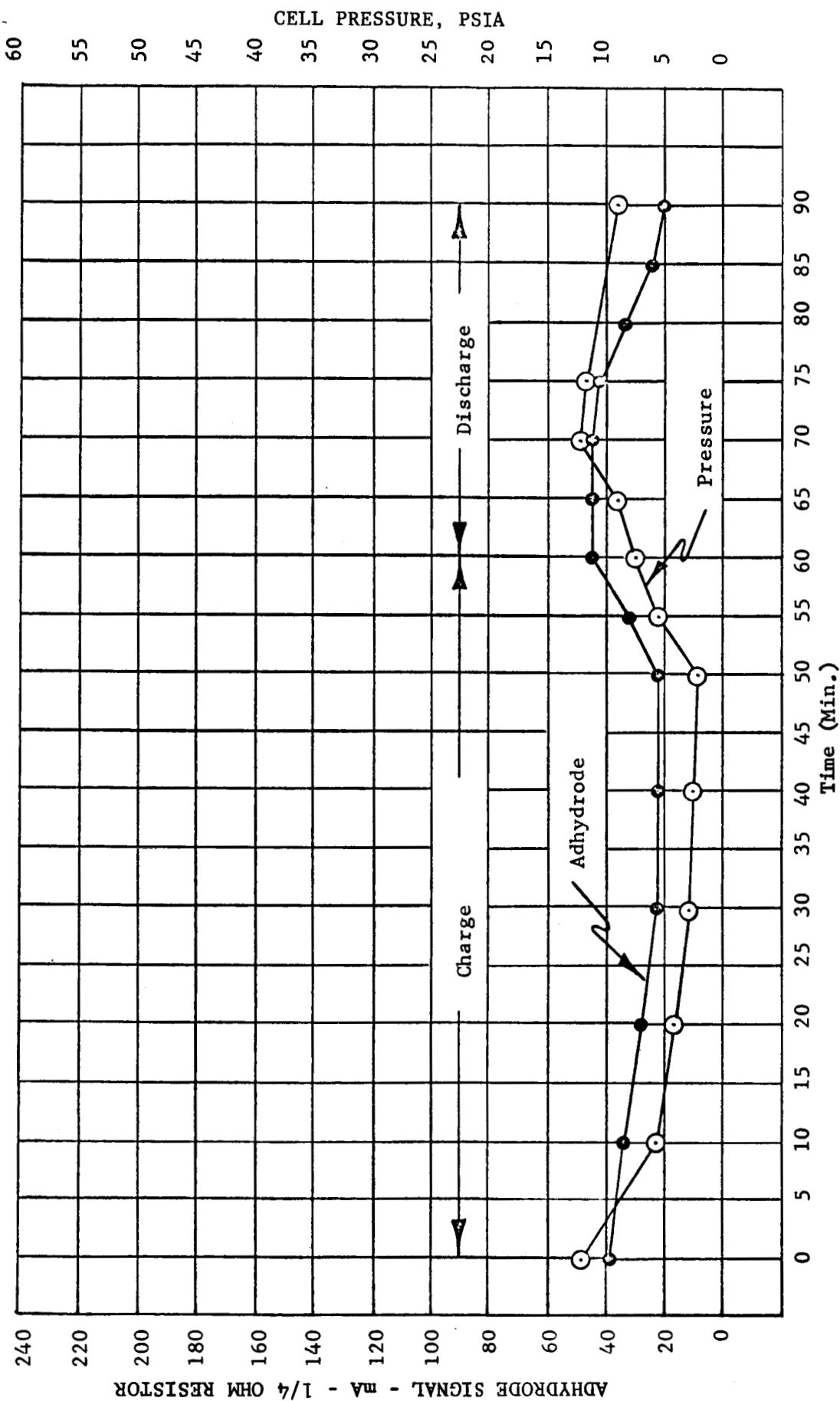
Figure 21- Cycle 65 Control Cell 50% DOD -20°C (-4°F)
14 A Discharge, 7.7 A Charge

4-1217

-35-

Figure 22- Cycle 3 Exp. Cell 50% DOD 0°C (32°F)

9 A Discharge, 5 A Charge

4-1218
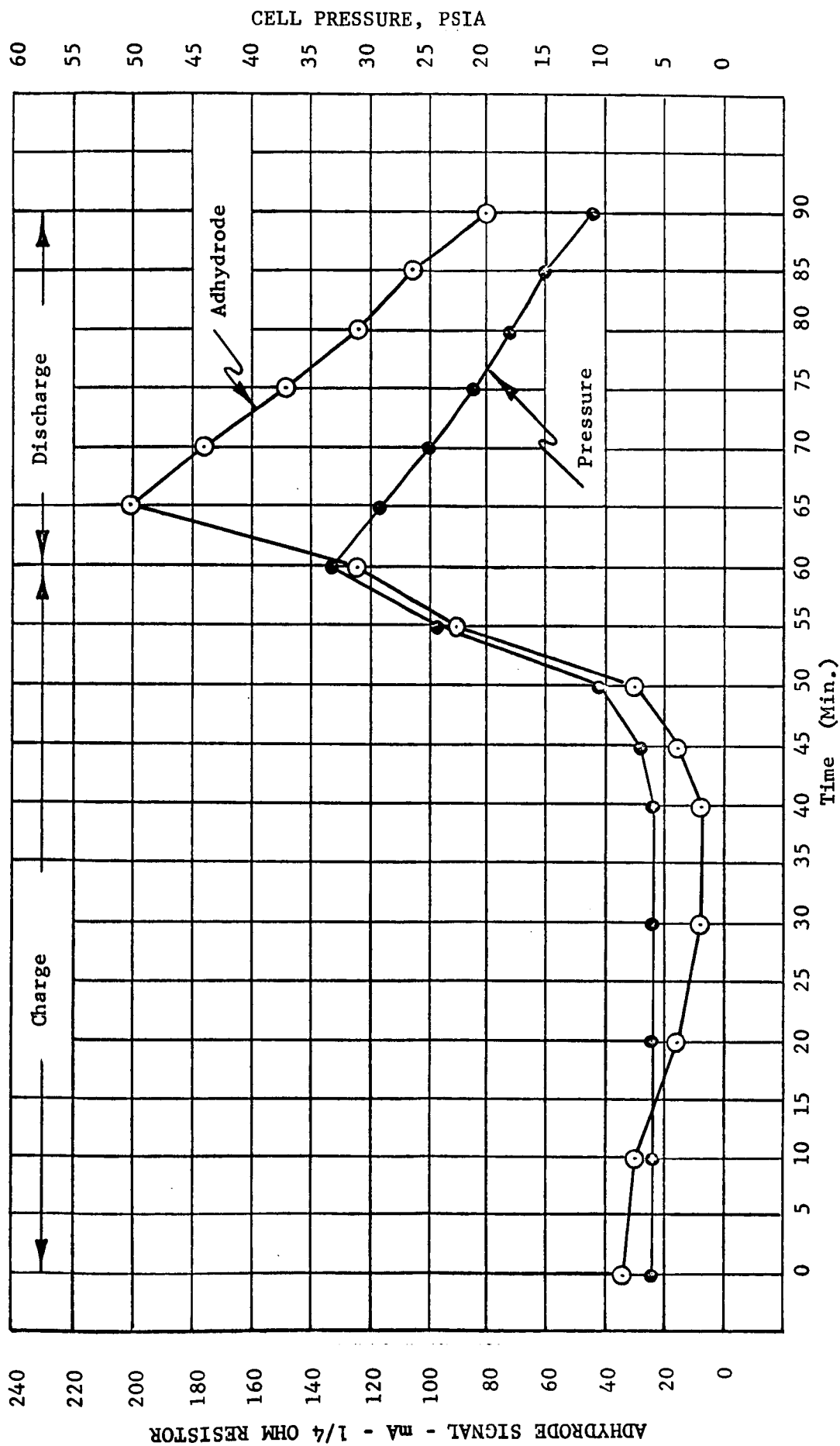
Figure 23- Cycle 3 Control Cell 50% DOD 0°C (32°F)
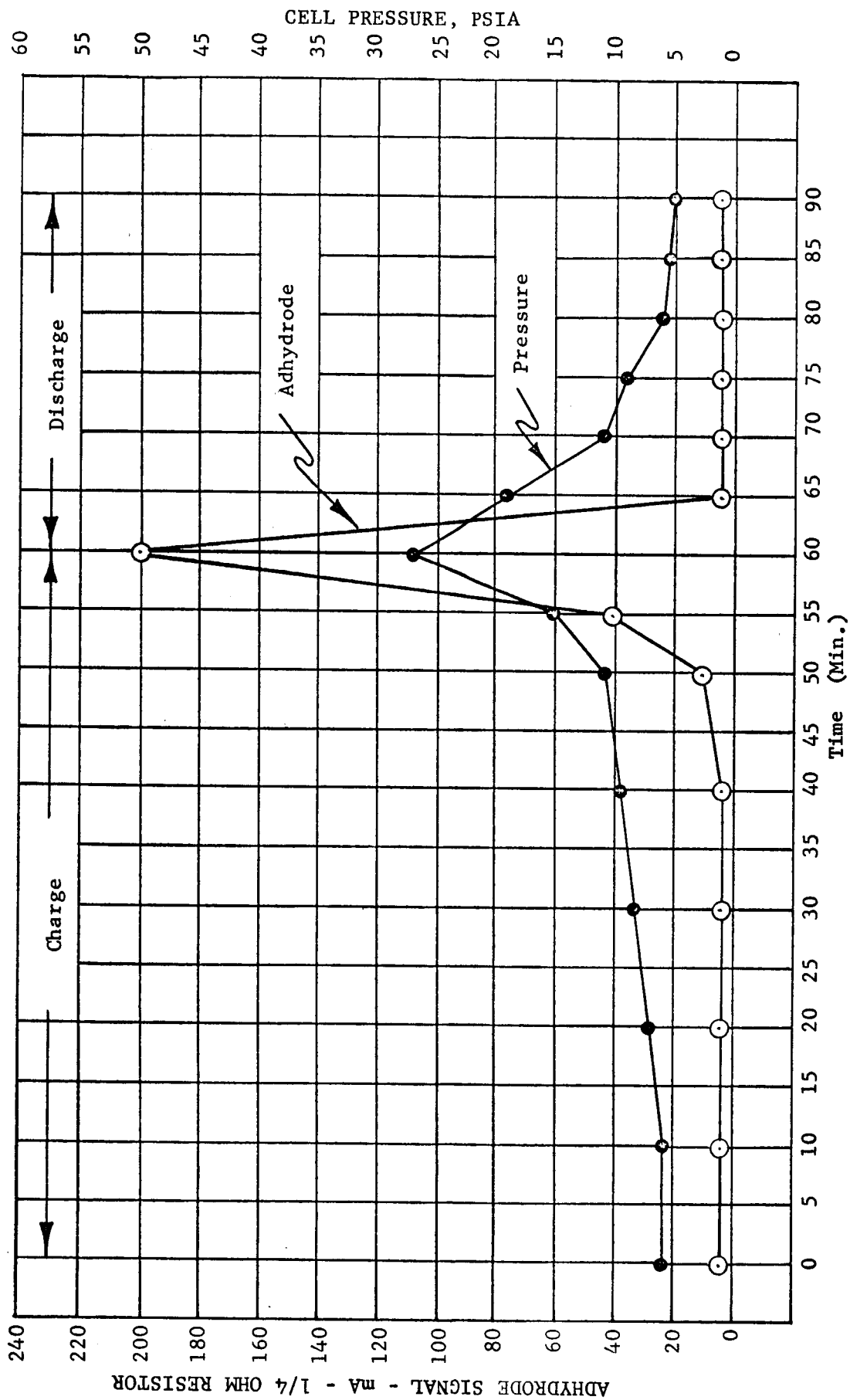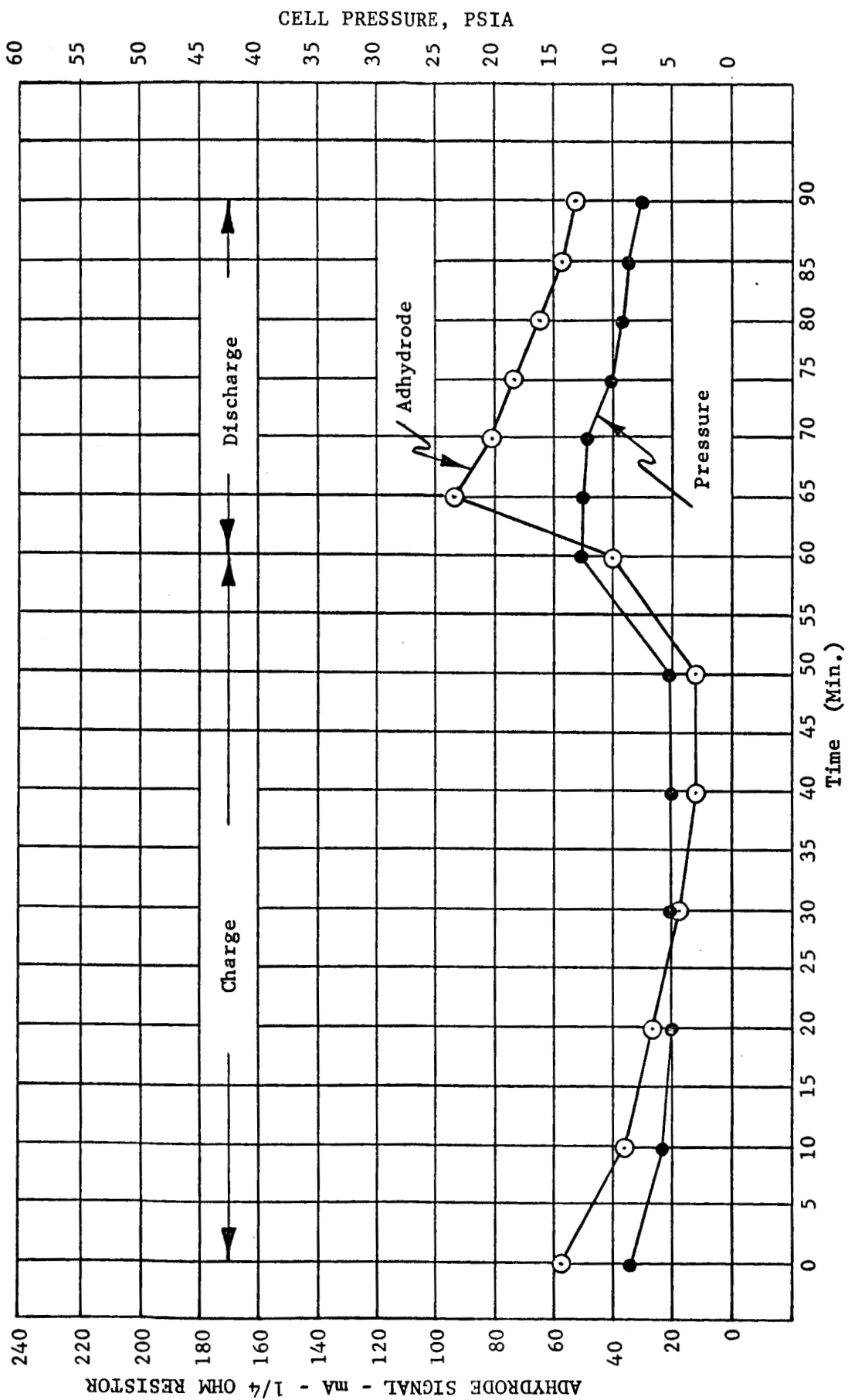14 A Discharge, 7.7 A Charge

Figure 24- Cycle 61 Exp. Cell 50% DOD 0°C (32°F)

9 A Discharge, 5 A Charge

Figure 25 - Cycle 61   Control Cell   50% DOD   0°C (32°F)
14 A Discharge, 7.7 A Charge

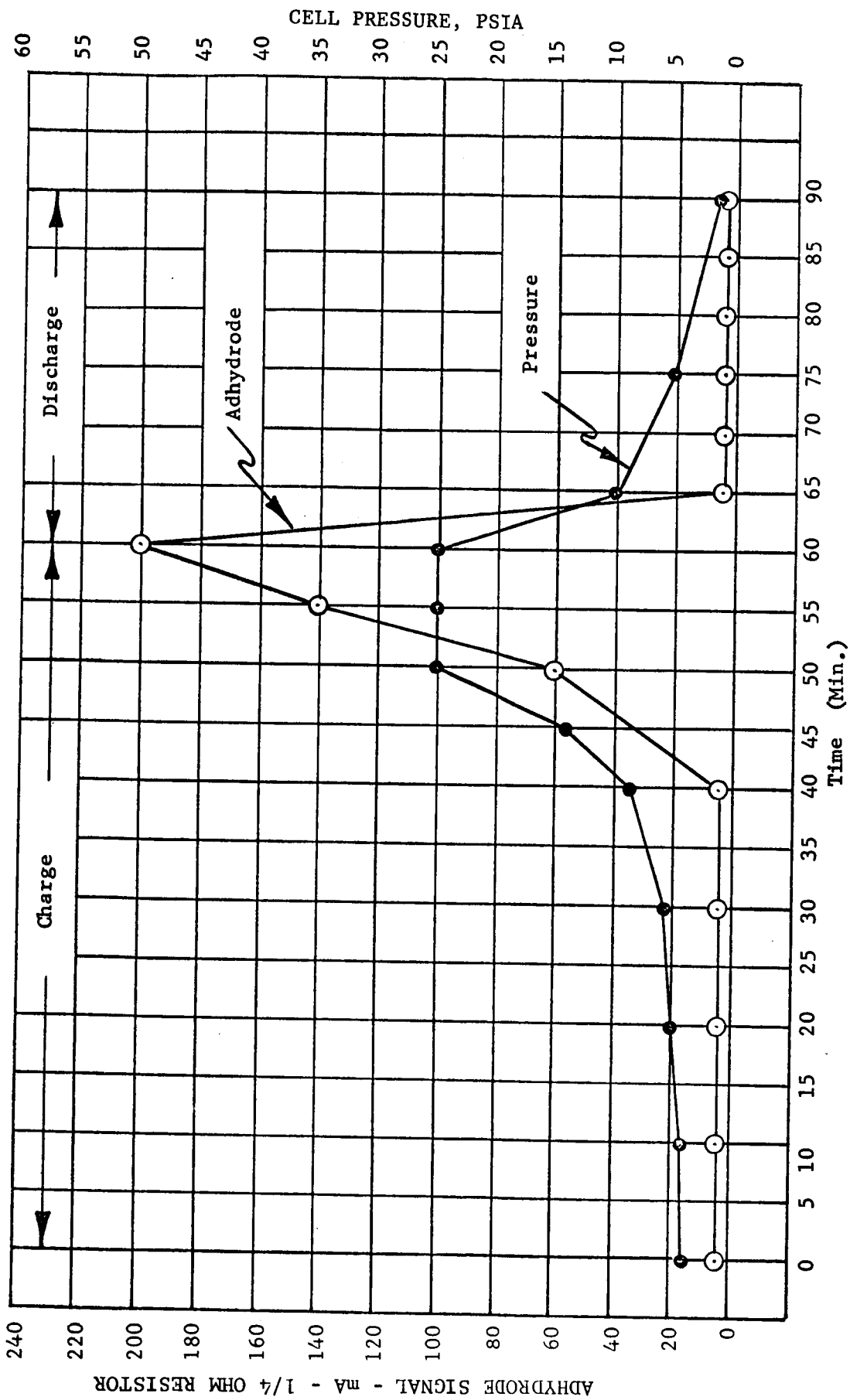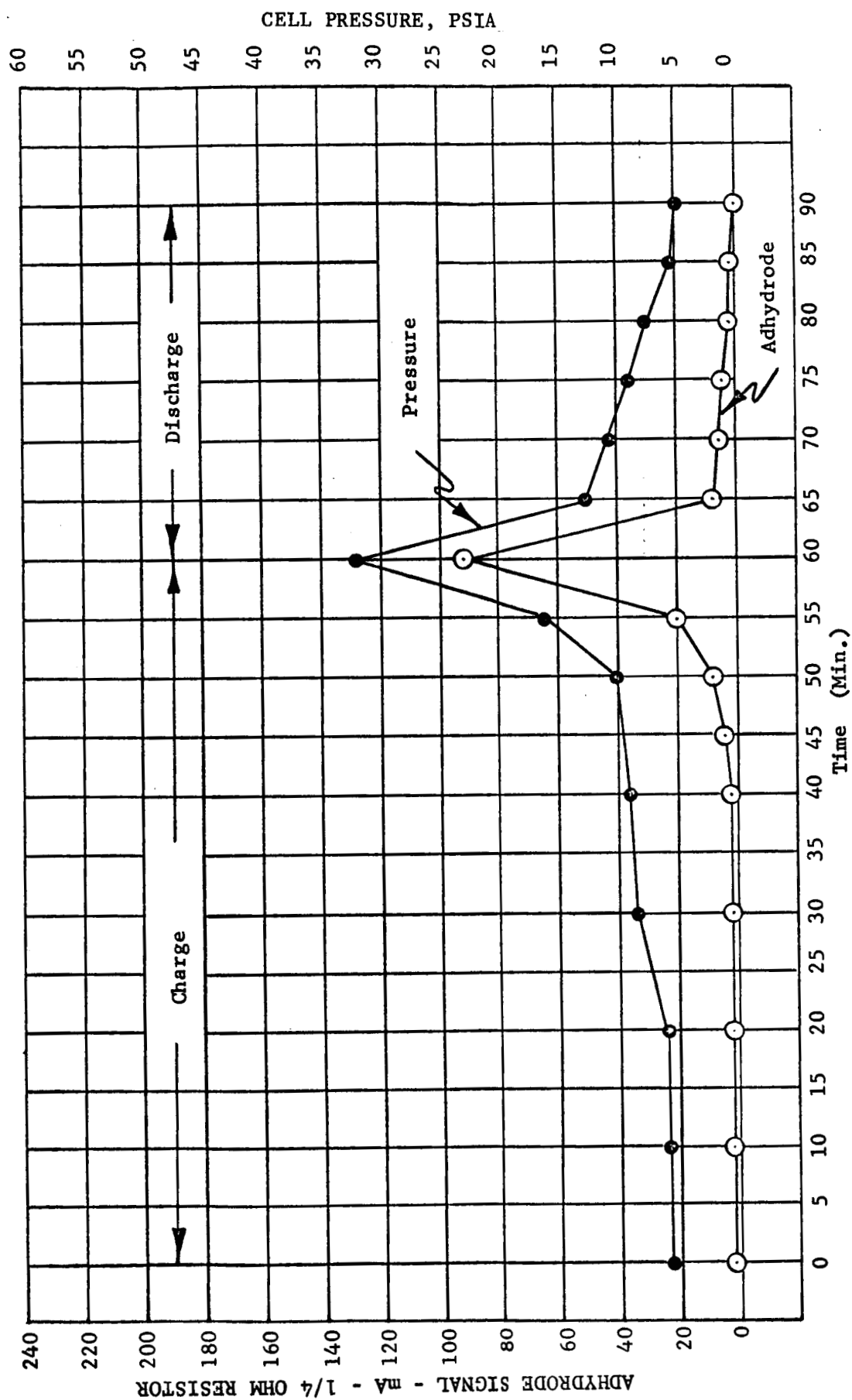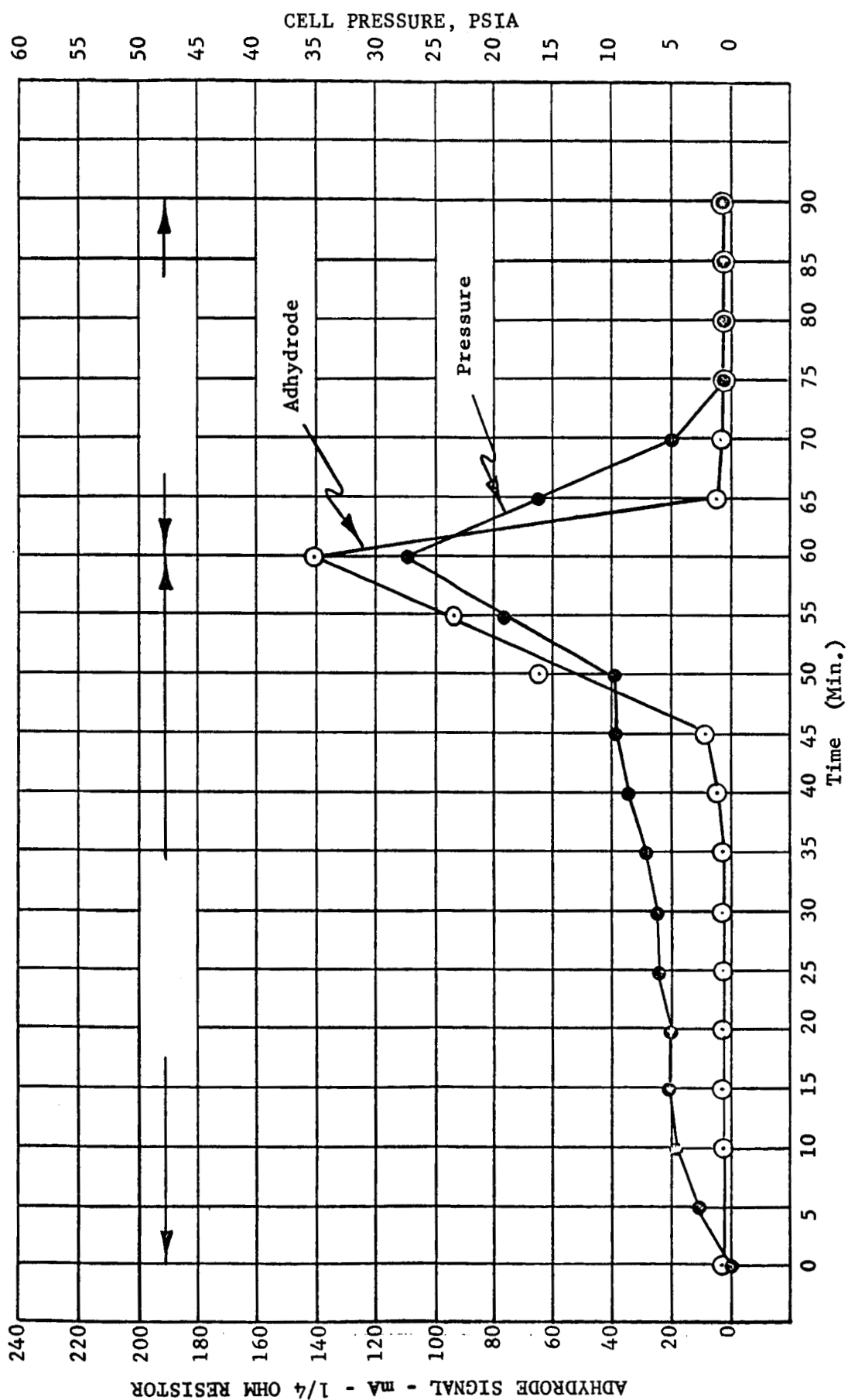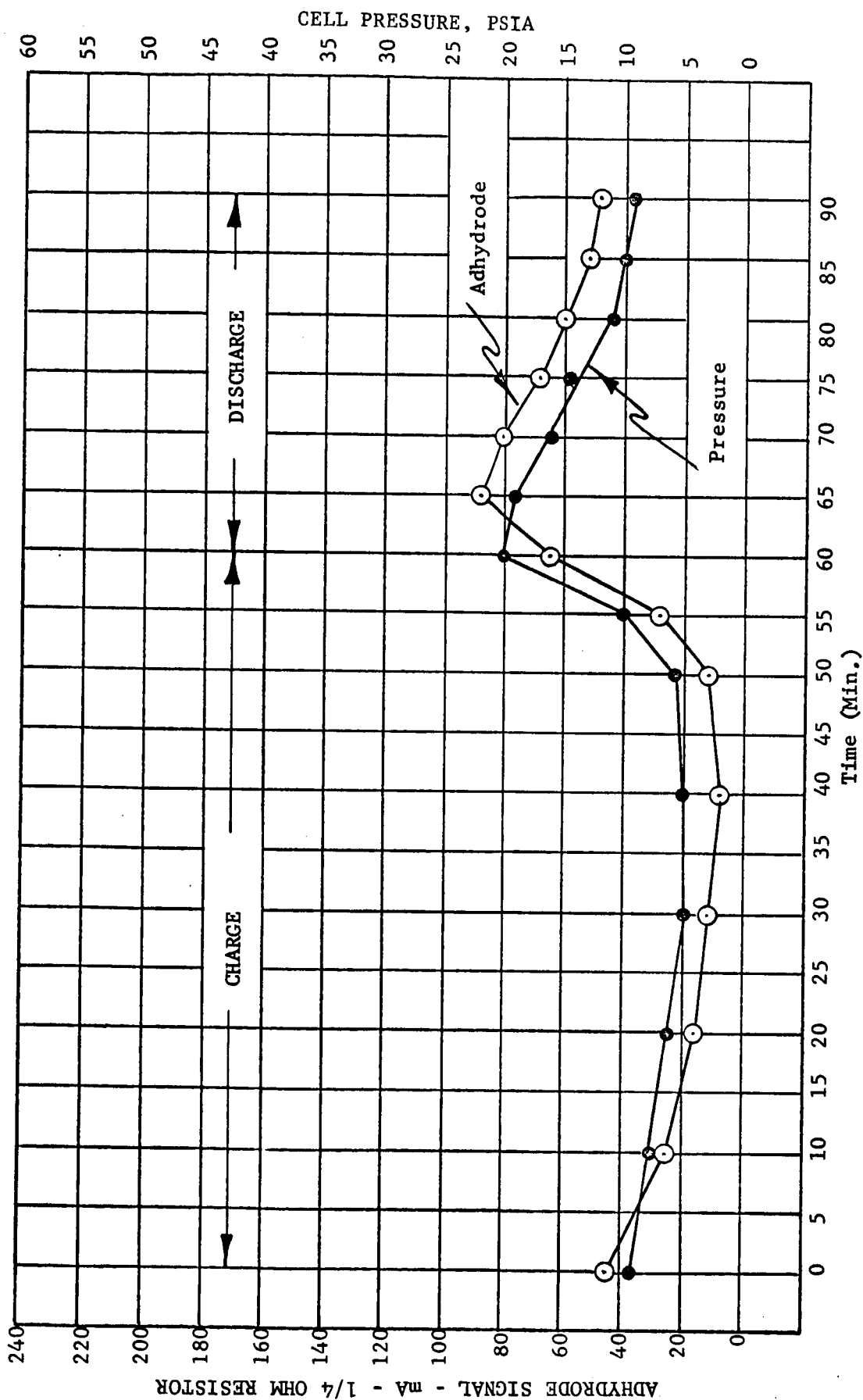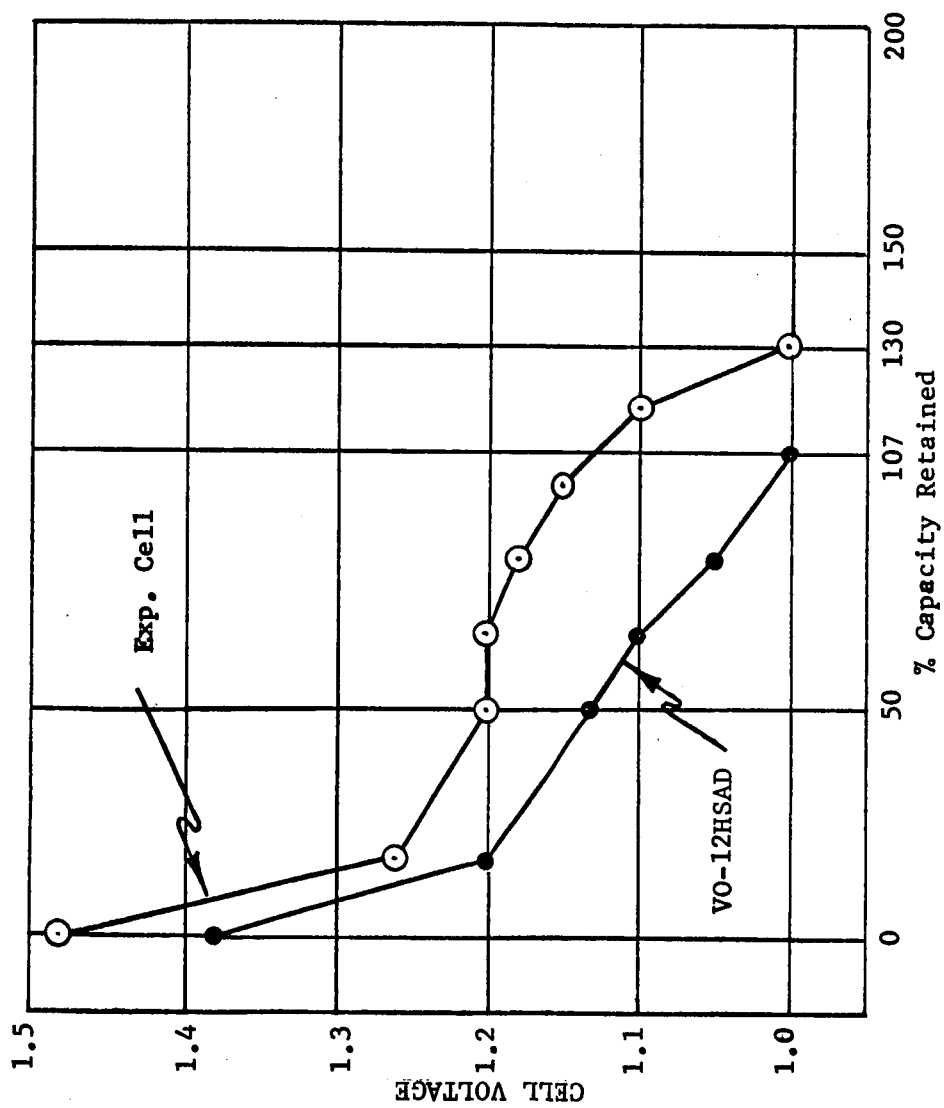FIGURE 26   TYPICAL CAPACITY AFTER 65 CYCLES, 50% DOD, AT -20°C (-40°F)
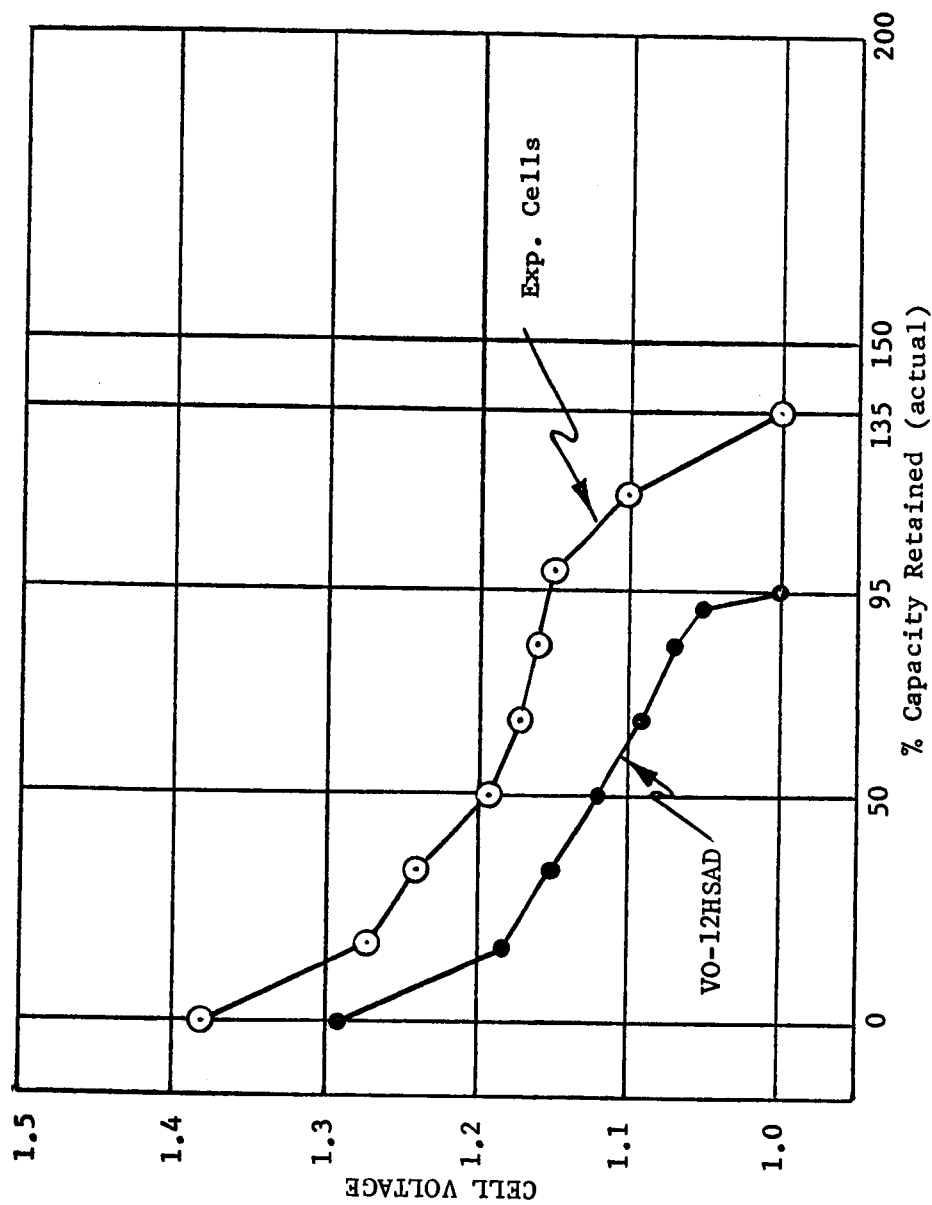DISCHARGED AT C/2

FIGURE 27. TYPICAL CAPACITY AFTER 61 CYCLES, 50% DOD, AT 0°C (32°F)
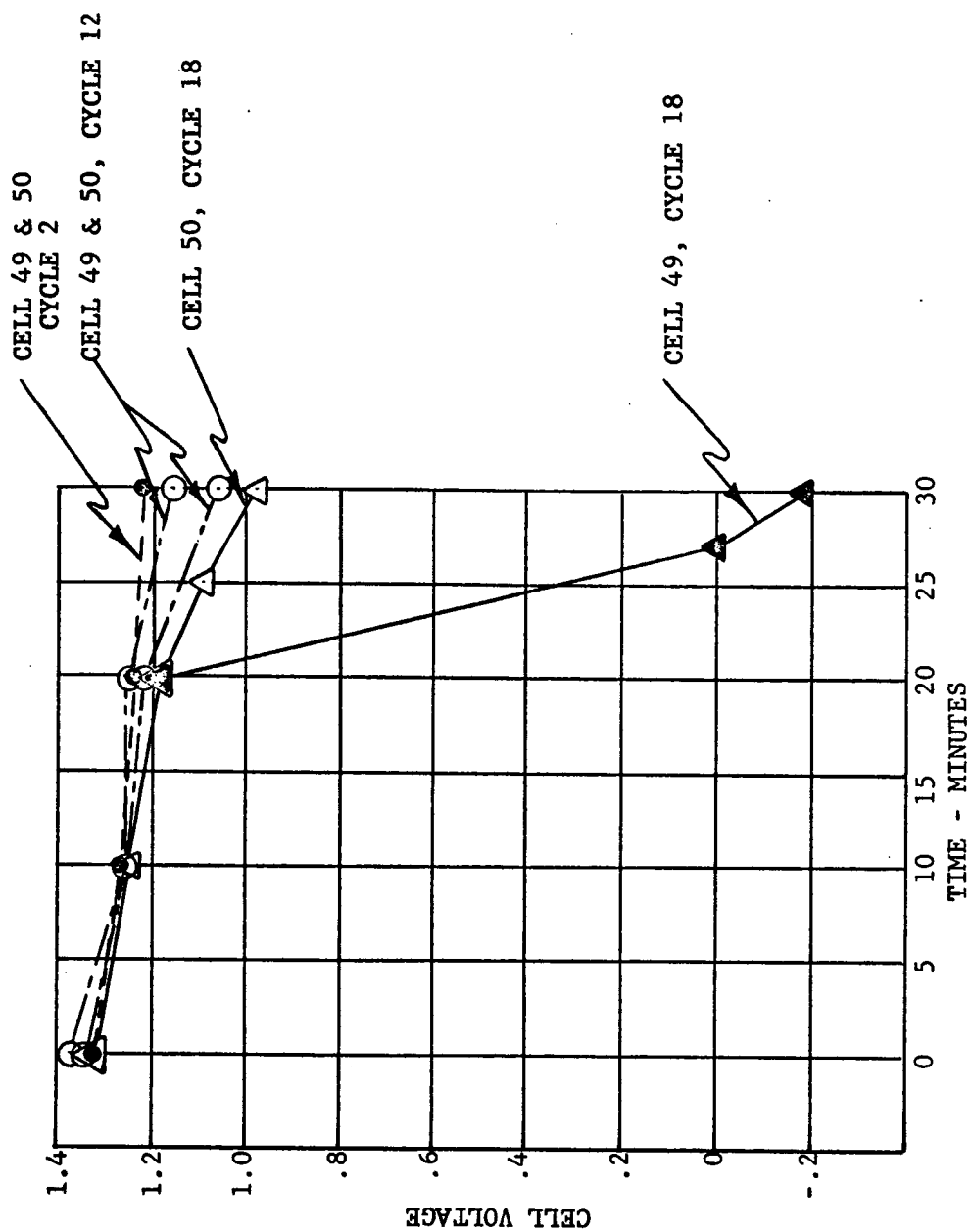DISCHARGED AT C/2

FIGURE 28   DISCHARGE PORTION OF CYCLES 2, 12, 18 -- 50% DOD, 35°C (95°F)

The cells were again placed in the oven at 40°C (104°F) and were cycled at a 10% depth of discharge for 10 days (158 cycles). Figure 29 is the pressure, Adhydrode and discharge curve for cycle 142. Figure 30 is the capacity of the two cells after cycling (nominal cell capacity is 10 Ah).

After completing the 10% depth of discharge cycling (first 158 cycles), the cells were cycled at 20, 30, and 25% depths of discharge. One hundred ninety-two cycles were completed at 20% depth of discharge and seventy at 30%. After this, the depth of discharge was reduced to 25% and a life test was conducted at this level. Figure 31 is the final cycle at 20% DOD. Figure 32 is a complete curve for cycle 707 at 25% DOD. Between the 710th and 750th cycle, the cell failed due to shorting.

Again, even though the cycle life was short, it has served to show that the four electrode concept is feasible and cells so equipped may be cycled with good charge control and low internal pressure.

c. Gassing Characteristics

In order to evaluate the gassing characteristics of the cells containing fuel cell electrodes, as compared to those cells containing a passive Adhydrode, the following test was performed.

Three cells containing fuel cell electrodes and three VO-12HSAD cells (the Adhydrode in the passive mode) were charged at C/2 to 25 psig (40 psia) at temperatures between -20°C (0°F) and 40°C (104°F). The results for a typical pair of cells are shown in Figures 33 and 34, and briefly summarized in Table VIII. It is evident from these results that the inclusion of a fuel cell electrode in a sealed cell permits wider latitude in the charge mode (i.e., higher rates for longer times with reduced probability of cell failure due to excessive pressure), and also aids in keeping the cell pressure at a low value.

TABLE VIII

PERCENT ACTUAL CAPACITY INPUT TO 40 PSIA
AT C/2, VERSUS TEMPERATURE

TEMPERATURE	VO-12HSAD	EXPERIMENTAL CELLS
-20°C (0°F)	108%	142%
0°C (32°F)	138%	158%
25°C (72°F)	79%	150%
40°C (100°F)	100%	150%

3. Low Rate Charging Characteristics

During testing of cells with fuel cell scavenger electrodes, it became apparent that when these cells were charged at a low rate (C/10), for 16-20 hours, from a dead shorted condition, and then subsequently discharged, the capacity of the cell fell far below the rated capacity. However, if the identical cells were charged at a high rate (C/2) to the same ampere-hour input, and then subsequently discharged, the capacities were significantly above the rated capacity. As a case in point, eleven VO-10HSADS (10 Ah capacity) cells yielded an average capacity of 7.33 Ah after a C/10 charge and 12.47 Ah after a C/2 charge.
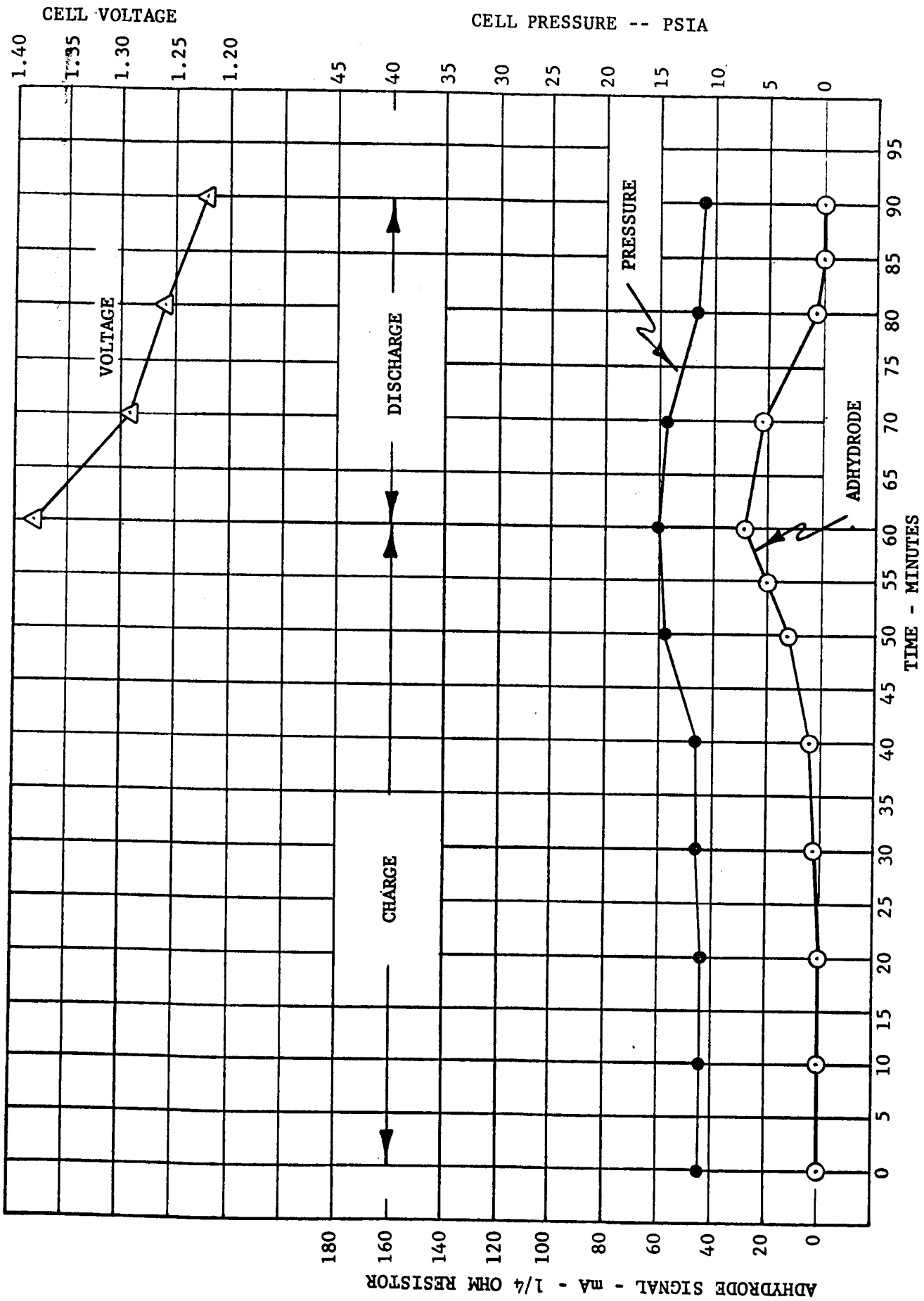
FIGURE 29 · ADHYDRODE SIGNAL, PRESSURE, & CELL VOLTAGE, CYCLE NO. 142
10% DOD, 40°C (100°F)

4-1508

-44-
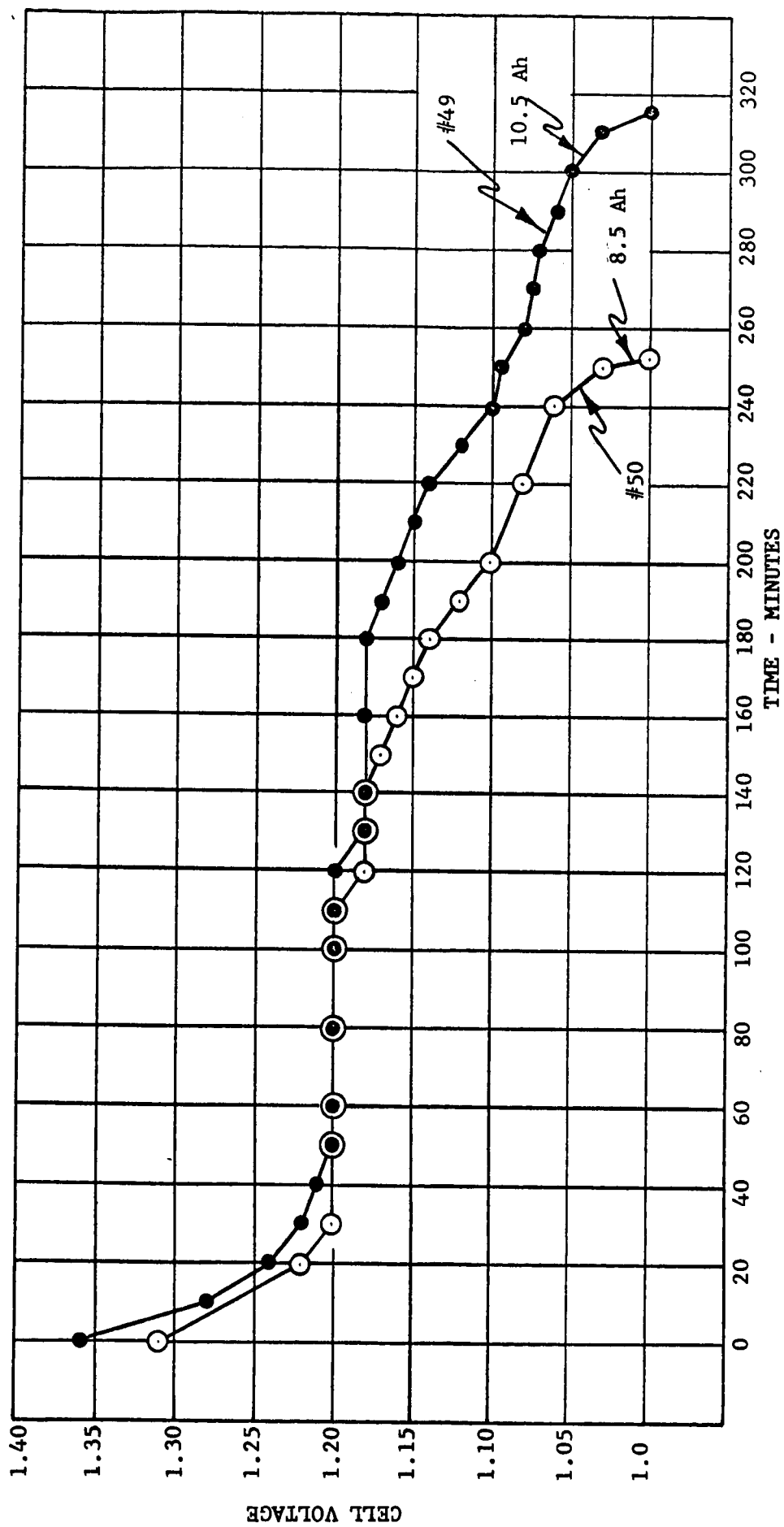
FIGURE 30   CAPACITY AFTER 158 CYCLES, 10% DOD, 40°C (104°F), C/5 DISCHARGE
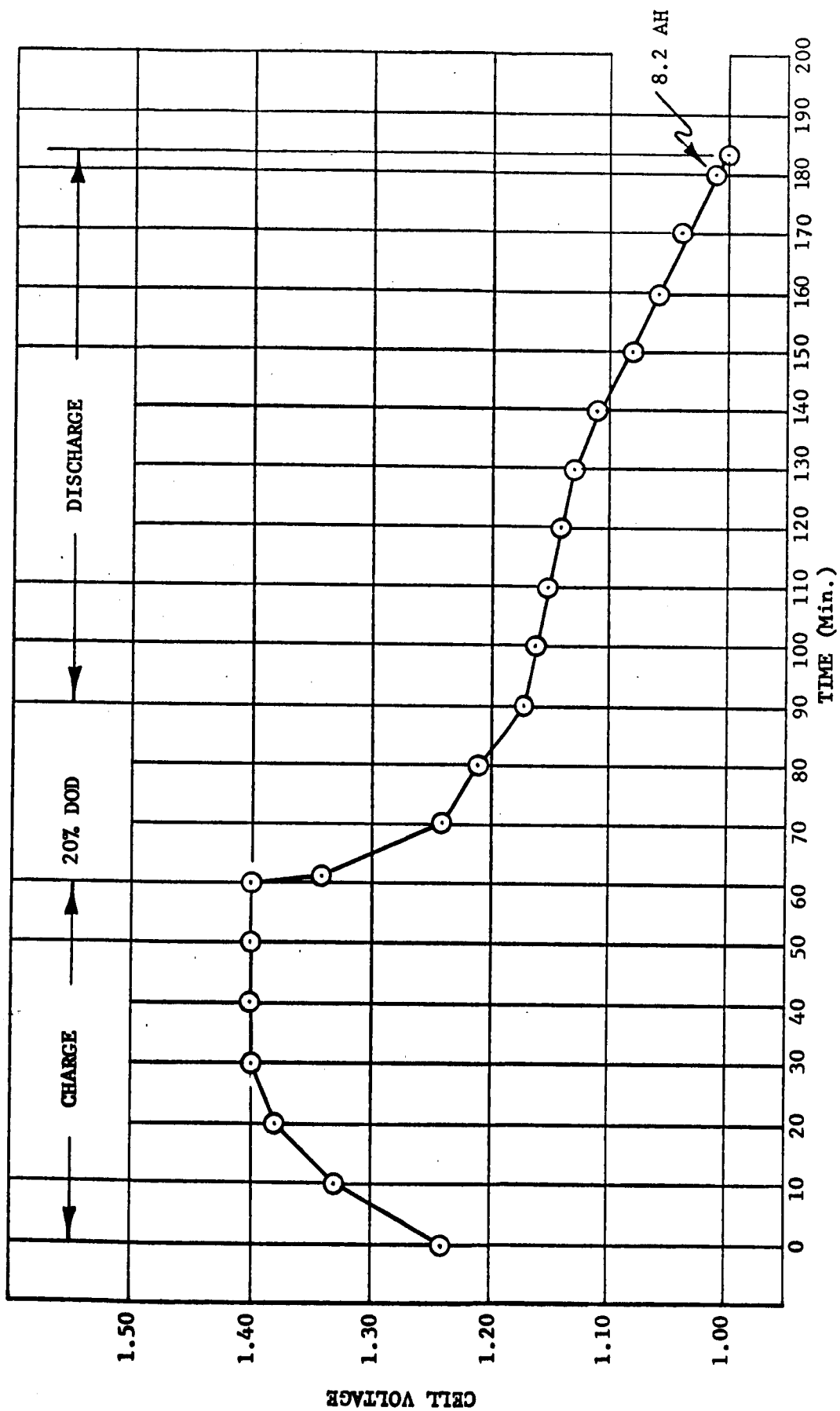
FIGURE 31   CYCLE 192 & CAPACITY DETERMINATION, 20% DOD, 40°C (104°F)

FIGURE 32   CYCLE 707, 25% DEPTH OF DISCHARGE, 40°C (100°F)

4-1558

-47-
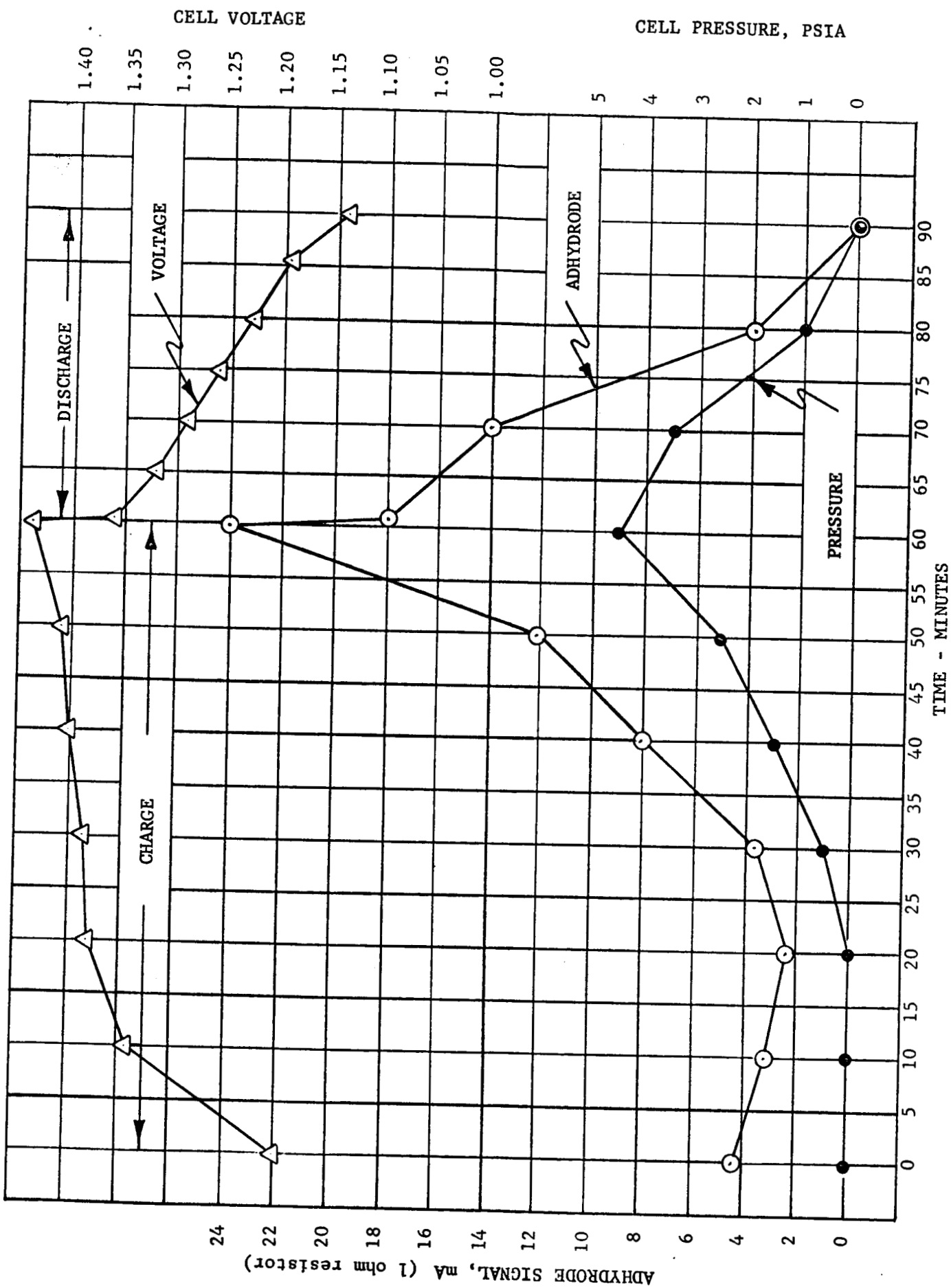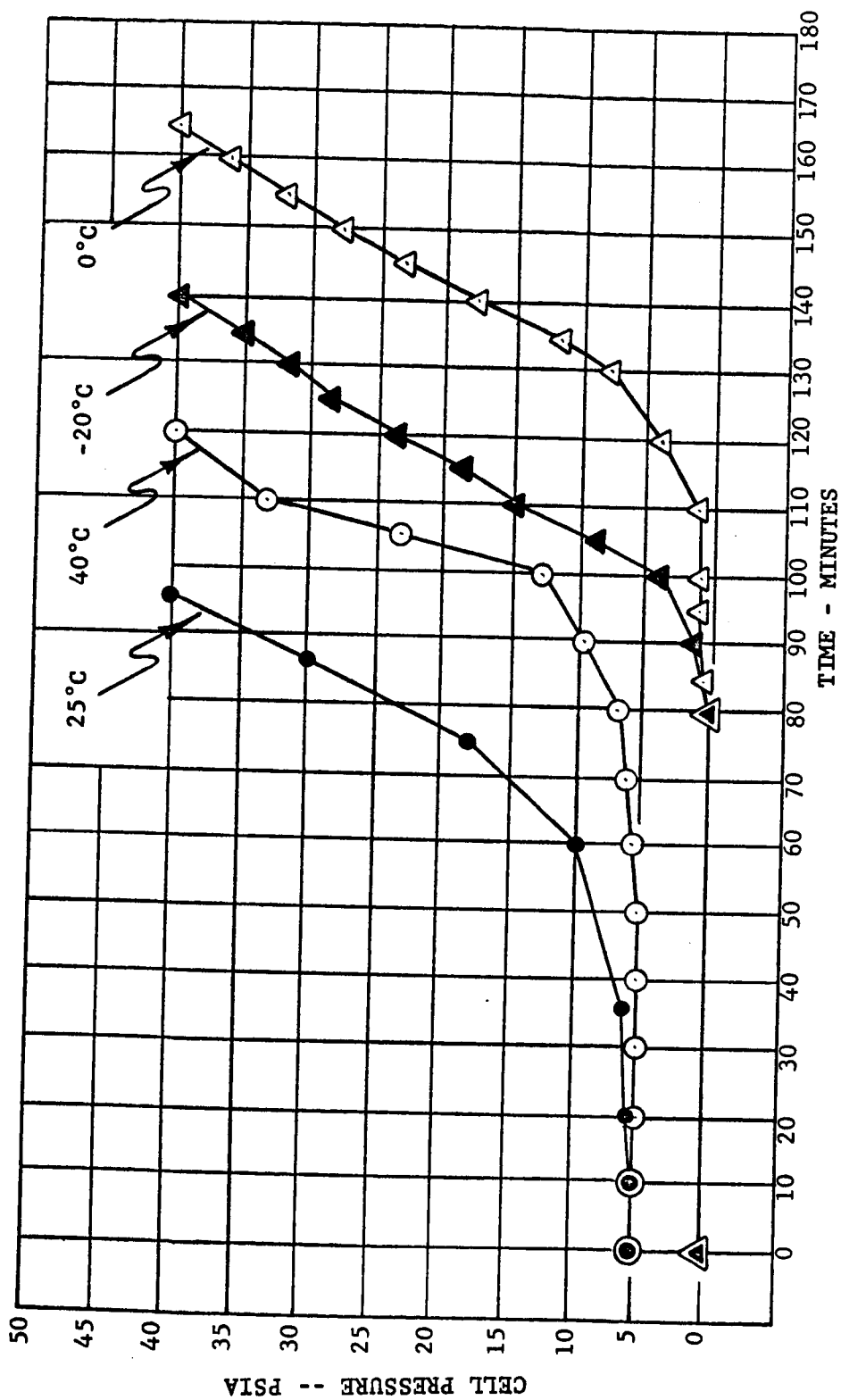
FIGURE 33   C/2 CHARGE TO 40 PSIA -- VO-12HSAD CELLS
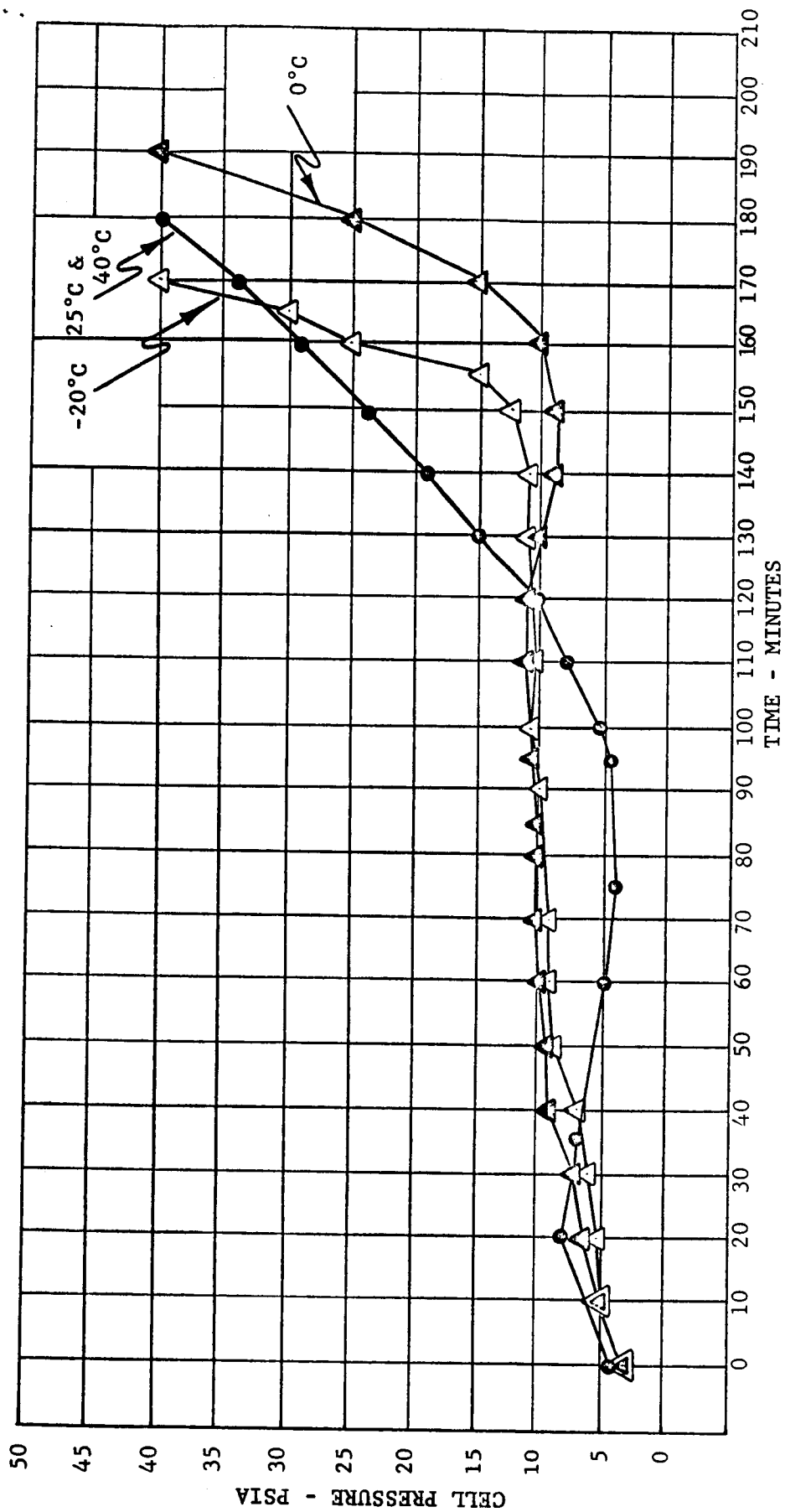
FIGURE 34   C/2 CHARGE TO 40 PSIA - EXPERIMENTAL CELLS WITH FUEL CELL ELECTRODES

4-1511

A clue to the reason for this behavior can be obtained by investigating internal cell pressure as a function of ampere-hour input. In a hermetically sealed cell of the VO type, (standard Gulton sealed cell) the end-of-charge pressure (C/10 rate for 24 hours) is usually between 20 and 35 psia. However, when a fuel cell electrode is included, the end-of-charge pressure is in the range of 5 to 10 psia. If we consider the reactions involved and apply Le Chatelier's principle, a correlation between the low cell pressure and low capacity may be obtained.

During charge and before overcharge, the pertinent reactions are:

$$4Ni(OH)_2 + 4OH^- \longrightarrow 4NiOOH + 4H_2O + 4e^- \qquad \text{Eq. (1)}$$

$$4OH^- \rightleftharpoons O_2 + 2H_2O + 4e^- \qquad \text{Eq. (2)}$$
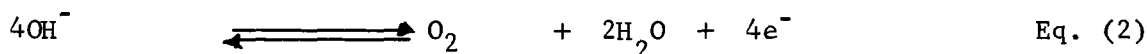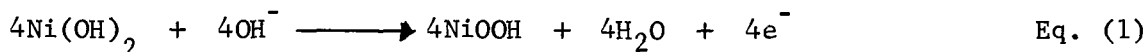
We must asseme that the oxygen evolution reaction is microscopically reversible, which, in principle, it is, otherwise the following analysis would not apply. Then we may say that at the onset of charge, the reactions are in competition. In the case of the standard VO type cell, there is a buildup of oxygen pressure which tends to suppress reaction (2) and allows reaction (1) to proceed efficiently. However, if, when a fuel cell electrode is included, the oxygen is recombined almost as fast as it is generated, the reactions continue to compete and the charging reaction (1) proceeds at a less efficient rate. Expressing the above in a mathematical form, we have from reaction (2):

$$\frac{dP_{O_2}}{dt} = k_f (P_{eq} - P_{O_2})$$

where P_{eq} is some equilibrium pressure and P_{O_2} is the instantaneous pressure.

The fraction of the total current producing the parasitic reaction (2) is:

$$i_{O_2} = A \frac{dP_{O_2}}{dt}$$

where: A   =   4FV/RT
         F   =   Faraday
         V   =   Cell (free) Volume, and
         R & T =   their usual meanings

$$i_{O_2} = Ak_f (P_{eq} - P_{O_2})$$

The total current, $I = i_{O_2} + i_a$

$$1 = \frac{i_{O_2}}{I} + \frac{i_a}{I}$$

$$\epsilon = \text{efficiency} = \frac{i_a}{I}$$

$$\epsilon = 1 - \frac{i_{O_2}}{I}$$

$$i_{O_2} \text{ max} = Ak_f P_{eq}$$

$$\epsilon_{min} = \frac{Ak_f P_{eq}}{I}$$

or the lower the instrantaneous pressure below the equilibrium value, the lower the charge efficiency.

V. CONCLUSIONS

The sensitivity of the Adhydrode material can be increased. The sensitivity increase is obtained at the expense of the mechanical properties. As a compromise in trade-off of properties, it was concluded to use the Adhydrode material as it existed prior to the start of this work.

The location of the Adhydrode within the cell had an effect upon its sensitivity. The best results, signal versus pressure, were obtained from Adhydrodes placed in the center of the electrode pack. This is the position selected for the signalling electrode.

Several materials were tested for use as scavenger electrodes. The best material investigated was a platinum bearing electrode developed for use in fuel cells. This material is purchased as AB6X from the American Cyanamid Company. It is connected directly to the negative electrode group, and located on the outside of the pack so that it can be in direct contact with the atmosphere of the cell.

Cells were fabricated using the significant findings in the first two phases of the program. These cells contained the Adhydrode in its most advantageous position, and the AB6X material in its most advantageous location. For use as controls, cells were made using the Adhydrode in the usual "U" shaped manner. It was found that:

(1) Four electrode cells do not exhibit an overshoot in the Adhydrode signal.

(2) Four electrode cells have a rapid signal decay.

(3) The scavenger electrode is sufficiently effective to permit a C/2 continuous overcharge at pressures not exceeding 50 PSIG.

(4) Recombination is independent of the composition of the atmosphere within the four electrode cells.

(5) At room temperature, 1600 cycles (800 consecutive) have been achieved on the four electrode cells.

(6) At low temperatures (-20° and 0°C), the four electrode cells had superior pressure and Adhydrode characteristics when compared to control cells.

(7) Cycling at 40°C (800 consecutive cycles) indicate that there is a 30% depth of discharge limitation.

VI. CONSTRUCTION OF BATTERIES FOR DELIVERY

Four, five-cell batteries have been delivered to NASA/Goddard in fulfillment of the contract requirements.

Each cell was constructed to contain 13 positive electrodes, 14 negative electrodes, 1 internally connected fuel cell scavenger electrode, and an Adhydrode connected to a third terminal. All plates are 70 mm^2 in area. All cells were equipped with pressure gauges. All cells were cycled three times, matched as closely as possible, fabricated into batteries, and then the battery capacity was determined to either 5 volts (1 volt/cell avg.) or to 0.5 volts on any one cell.

Battery	Capacity
1	12.00
2	11.83
3	12.40
4	12.25

OFFICIAL DISTRIBUTION LIST
FOR BATTERY REPORTS

May 1, 1967

National Aeronautics & Space Admin.
Scientific and Technical Information
  Facility
College Park, Maryland 20740
Attn: NASA Representative
Send 2 copies plus 1 reproducible

National Aeronautics & Space Admin.
Washington, D.C. 20546
Attn: RNW/E. M. Cohn

National Aeronautics & Space Admin.
Washington, D.C. 20546
Attn: FC/A. M. Greg Andrus

National Aeronautics & Space Admin.
Goddard Space Flight Center
Greenbelt, Maryland 20771
Attn: Gerald Halpert, Code 735

National Aeronautics & Space Admin.
Goddard Space Flight Center
Greenbelt, Maryland 20771
Attn: Thomas Hennigan, Code 716.2
Send 3 copies

National Aeronautics & Space Admin.
Goddard Space Flight Center
Greenbelt, Maryland 20771
Attn: Joseph Sherfey, Code 735

National Aeronautics & Space Admin.
Langley Research Center
Instrument Research Division
Hampton, Virginia 23365
Attn: John L. Patterson, MS-234

National Aeronautics & Space Admin.
Langley Research Center
Instrument Research Division
Hampton, Virginia 23365
Attn: M. B. Seyffert, MS 112

National Aeronautics & Space Admin.
Lewis Research Center
21000 Brookpark Road
Cleveland, Ohio 44135
Attn: N. D. Sanders, MS 302-1

National Aeronautics & Space Admin.
Lewis Research Center
21000 Brookpark Road
Cleveland, Ohio 44135
Attn: M. J. Saari, MS 500-202

National Aeronautics & Space Admin.
Lewis Research Center
21000 Brookpark Road
Cleveland, Ohio 44135
Attn: R. R. Miller, MS 500-202

National Aeronautics & Space Admin.
Geo. C. Marshall Space Flight Center
Huntsville, Alabama 35812
Attn: Philip Youngblood

National Aeronautics & Space Admin.
Geo. C. Marshall Space Flight Center
Huntsville, Alabama 35812
Attn: Richard Boehme
     Bldg. 4487-BB

National Aeronautics & Space Admin.
Manned Spacecraft Center
Houston, Texas 77058
Attn: William R. Dusenbury
Propulsion & Energy Systems Branch
Bldg. 16, Site 1

National Aeronautics & Space Admin.
Manned Spacecraft Center
Houston, Texas 77058
Attn: Richard Ferguson (EP-5)

National Aeronautics & Space Admin.
Manned Spacecraft Center
Houston, Texas 77058
Attn: Mr. Barry Trout

National Aeronautics & Space Admin.
Manned Spacecraft Center
Houston, Texas 77058
Attn: Forrest E. Eastman (EE-4)

National Aeronautics & Space Admin.
Washington, D.C. 20546
Attn: Office of Technology
  Utilization

National Aeronautics & Space Admin.
Ames Research Center
Pioneer Project
Moffett Field, California 94035
Attn: Arthur Wilbur/A. S. Hertzog

National Aeronautics & Space Admin.
Ames Research Center
Moffett Field, California 94035
Attn: Jon Rubenzer
    Biosatellite Project

National Aeronautics & Space Admin.
Electronics Research Center
575 Technology Square
Cambridge, Mass. 02139
Attn: Dr. Sol Gilman

Jet Propulsion Laboratory
4800 Oak Grove Drive
Pasadena, California 91103
Attn: Mr. Aiji Uchiyama

Department of the Army

U. S. Army Engineer R&D Labs.
Fort Belvoir, Virginia 22060
Electrical Power Branch
Energy Conversion Research Lab.

Commanding General
U. S. Army Weapons Command
Attn: AMSWE-RDR, Mr. G. Reinsmith
Rock Island Arsenal
Rock Island, Illinois 61201

U. S. Army Natick Laboratories
Clothing and Organic Materials Div.
Natick, Massachusetts 01760
Attn: G. A. Spano

Commanding Officer
U. S. Army Electronics R&D Labs.
Power Sources Division
Fort Monmouth, New Jersey 07003
Attn: Code SELRA/PS

Harry Diamond Laboratories
Room 300, Building 92
Conn. Ave. & Van Ness Street, N. W.
Washington, D.C. 20438
Attn: Nathan Kaplan

Department of the Navy

Office of Naval Research
Washington, D.C. 20360
Attn: Head, Power Branch, Code 429

Naval Research Laboratory
Washington, D.C. 20390
Attn: Dr. J. C. White, Code 6160

2

U. S. Navy
Special Projects Division
Marine Engineering Laboratory
Annapolis, Maryland 21402
Attn: J. H. Harrison

Naval Air Systems Command
Department of the Navy
Washington, D.C. 20360
Attn: Milton Knight (Code AIR-340C)

Commanding Officer
(Code QEWE, E. Bruess/H. Schultz)
U. S. Naval Ammunition Depot
Crane, Indiana 47522

Naval Ordnance Laboratory
Department of the Navy
Corona, California 91720
Attn: William C. Spindler (Code 441)

Naval Ordnance Laboratory
Silver Spring, Maryland 20910
Attn: Philip B. Cole (Code 232)

Commander, Naval Ship Sys. Command
Department of the Navy
Washington, D.C. 20360
Attn: C. F. Viglotti (Code 66605)

Commander, Naval Ship Sys. Command
Department of the Navy
Washington, D.C. 20360
Attn: Bernard B. Rosenbaum
(Code 03422)

Department of the Air Force

Flight Vehicle Power Branch
Aero Propulsion Laboratory
Wright-Patterson AFB, Ohio 45433
Attn: James E. Cooper

AF Cambridge Research Lab.
Attn: CRE
L. G. Hanscom Field
Bedford, Massachusetts 01731
Attn: Francis X. Doherty
Edward Raskind (Wing F)

Rome Air Development Center, ESD
Attn: Frank J. Mollura (RASSM)
Griffis AFB, New York 13442

Other Government Agencies

National Bureau of Standards
Washington, D.C. 20234
Attn: Dr. W. J. Hamer

National Bureau of Standards
Washington, D.C. 20234
Attn: Dr. A. Brenner

Office, Sea Warfare System
The Pentagon
Washington, D.C. 20310
Attn: G. B. Wareham

Mr. Donald A. Hoatson
Army Reactors, DRD
U. S. Atomic Energy Commission
Washington, D.C. 20545

Bureau of Mines
4800 Forbes Avenue
Pittsburgh, Pennsylvania 15213
Attn: Dr. Irving Wender

Private Organizations

Aerojet-General Corporation
Chemical Products Division
Azusa, California 91702
Attn: William H. Johnson

3

Aeronutronic Division of Philco Corp.
Technical Information Services
Ford Road
Newport Beach, California 92663

Aerospace Corporation
P. O. Box 95085
Los Angeles, California 90045
Attn: Library Acquisition Group

Allis-Chalmers Mfg. Co.
1100 South 70th Street
Milwaukee, Wisconsin 53201
Attn: Dr. P. Joyner

A. M. F.
Attn: Dr. Lloyd H. Shaffer
689 Hope Street
Springdale, Connecticut 06879

American University
Mass. & Nebraska Avenue, N. W.
Washington, D.C. 20016
Attn: Dr. R. T. Foley,
    Chemistry Department

Arthur D. Little, Inc.
Acorn Park
Cambridge, Massachusetts 02140
Attn: Dr. Ellery W. Stone

Atomics International Division
North American Aviation, Inc.
8900 De Sota Avenue
Canoga Park, California 91304
Attn: Dr. H. L. Recht

Battelle Memorial Institute
505 King Avenue
Columbus, Ohio 43201
Attn: Dr. C. L. Faust

Bell Laboratories
Murray Hill, New Jersey 07971
Attn: U. B. Thomas

Bell Telephone Laboratories, Inc.
Whippany, N. J. 07981
Attn: D. O. Feder, Room 3B-294

The Boeing Company
P. O. Box 3868
Seattle, Washington 98124
Attn: Sid Gross, MS 85-86

Borden Chemical Company
Central Research Lab.
P. O. Box 9524
Philadelphia, Pennsylvania 19124

Burgess Battery Company
Foot of Exchange Street
Freeport, Illinois 61033
Attn: Dr. Howard J. Strauss

C & D Batteries
Division of Electric Autolite Co.
Conshohocken, Pennsylvania 19428
Attn: Dr. Eugene Willihnganz

Calvin College
Grand Rapid, Michigan 49506
Attn: Prof. T. P. Dirkse

Catalyst Research Corporation
6101 Falls Road
Baltimore, Maryland 21209
Attn: H. Goldsmith

ChemCell Inc.
150 Dey Road
Wayne, New Jersey 07470
Attn: Peter D. Richman

4

G. & W. H. Corson, Inc.
Plymouth Meeting
Pennsylvania 19462
Attn: Dr. L. J. Minnick

Cubic Corporation
9233 Balboa Avenue
San Diego, California 92123
Attn: Librarian
    Mrs. Judy Kalak

Delco Remy Division
General Motors Corporation
2401 Columbus Avenue
Anderson, Indiana 46011
Attn: Dr. J. J. Lander

Douglas Aircraft Company, Inc.
Astropower Laboratory
2121 Campus Drive
Newport Beach, California 92663
Attn: Dr. George Moe

Dynatech Corporation
17 Tudor Street
Cambridge, Massachusetts 02139
Attn: R. L. Wentworth

E. I. DuPont De Nemours & Co.
Explosives Department
Repauno Development Laboratory
Gibbstown, New Jersey 08027
Attn: Mr. R. W. Prugh
    (Contract NASw-1233)

Eagle-Picher Company
Post Office Box 47
Joplin, Missouri 64801
Attn: E. P. Broglio

Electric Storage Battery Co.
Missile Battery Division
2510 Louisburg Rd.
Raleigh, North Carolina 27604
Attn: A. Chreitzberg

Electric Storage Battery Co.
Carl F. Norberg Research Center
19 West College Avenue
Yardley, Pennsylvania 19067
Attn: Dr. R. A. Schaefer

Electrochimica Corporation
1140 O'Brien Drive
Menlo Park, California 94025
Attn: Dr. Morris Eisenberg

Electro-Optical Systems, Inc.
300 North Halstead
Pasadena, California 91107
Attn: Martin Klein

Emhart Corp
Box 1620
Hartford, Connecticut 06102
Attn: Dr. W. P. Cadogan

Engelhard Industries, Inc.
497 DeLancy Street
Newark, New Jersey 07105
Attn: Dr. J. G. Cohn

Dr. Arthur Fleischer
466 South Center Street
Orange, New Jersey 07050

General Electric Company
Schenectady, New York 12301
Attn: Dr. R. C. Osthoff/Dr. W. Carson
    Advanced Technology Lab.

General Electric Company
Missile & Space Division
Spacecraft Department
P. O. Box 8555
Philadelphia, Pennsylvania 19101
Attn: E. W. Kipp, Room U-2307

5

General Electric Company
Battery Products Section
P. O. Box 114
Gainsville, Florida 32601
Attn: W. H. Roberts

General Electric Company
Research and Development Center
P. O. Box 8
Schenectady, New York 12301
Attn: Dr. H. Liebhafsky

General Motors-Defense Research Labs.
6767 Hollister Street
Santa Barbara, California 93105
Attn: Dr. J. S. Smatko/Dr. C. R. Russell

Globe-Union, Incorporated
P. O. Box 591
Milwaukee, Wisconsin 53201
Attn: Mr. J. D. Onderdonk
        V. P. Marketing

Gould-National Batteries, Inc.
Engineering & Research Center
(Dr. D. Douglas)
2630 University Avenue, S. E.
Minneapolis, Minnesota 55418

Gulton Industries
Alkaline Battery Division
212 Durham Avenue
Metuchen, New Jersey 08840
Attn: Dr. Robert Shair

Gulton Industries
Alkaline Battery Division
212 Durham Avenue
Metuchen, New Jersey 08840
Attn: H. N. Seiger
        Contract NAS W-12,300 only

Hughes Aircraft Corporation
Centinda Ave. & Teale Street
Culver City, California 90230
Attn: T. V. Carvey

Hughes Aircraft Corporation
Bldg. 366, M. S. 524
El Segundo, California 90245
Attn: P. C. Ricks

IIT Research Institute
10 West 35th Street
Chicago, Illinois 60616
Attn: Dr. H. T. Francis

Institute for Defense Analyses
R&E Support Division
400 Army-Navy Drive
Arlington, Virginia 22202
Attn: Mr. R. Hamilton

Institute for Defense Analyses
R&E Support Division
400 Army-Navy Drive
Arlington, Virginia 22202
Attn: Dr. G. Szego

Idaho State University
Department of Chemistry
Pocatello, Idaho 83201
Attn: Dr. G. Myron Arcand

Institute of Gas Technology
State and 34th Street
Chicago, Illinois 60616
Attn: B. S. Baker

International Nickel Co.
1000-16th Street, N. W.
Washington, D.C. 20036
Attn: Wm. C. Mearns

6

Johns Hopkins University
Applied Physics Laboratory
8621 Georgia Avenue
Silver Spring, Maryland 20910
Attn: Richard E. Evans

Johns Hopkins University
Applied Physics Laboratory
8621 Georgia Avenue
Silver Spring, Maryland 20910
Attn: Mr. Louis Wilson

Leesona Moos Laboratories
Lake Success Park, Community Drive
Great Neck, New York 11021
Attn: Dr. H. Oswin

Livingston Electronic Corporation
Route 309
Montgomeryville, Pa. 18936
Attn: William F. Meyers

Lockheed Missiles & Space Company
Technical Information Center
3251 Hanover Street
Palo Alto, California 93404

Mallory Battery Company
Broadway & Sunnyside Lane
North Tarrytown, New York 10591
Attn: R. R. Clune

P. R. Mallory & Co., Inc.
Northwest Industrial Park
Burlington, Massachusetts 01803
Attn: Dr. Per Bro

P. R. Mallory & Co., Inc.
3029 E. Washington Street
Indianapolis, Indiana 46206
Attn: Technical Librarian

Martin Company
Denver Division
(P1001, Mr. R. C. Wildman)
Mail No. P-6700-1
Denver, Colorado 80201

Martin Company
Electronics Research Department
P. O. Box #179
Denver, Colorado 80201
Attn: William B. Collins, MS 1620

Mauchly Systems, Inc.
Fort Washington Industrial Park
Fort Washington, Pennsylvania
Attn: John H. Waite

Melpar
Technical Information Center
7700 Arlington Blvd.
Falls Church, Virginia 22046

Metals and Controls Division
Texas Instruments, Inc.
34 Forrest Street
Attleboro, Massachusetts 02703
Attn: Dr. E. M. Joe

Midwest Research Institute
425 Volker Boulevard
Kansas City, Missouri 64110
Attn: Physical Science Laboratory

Monsanto Research Corporation
Everett, Massachusetts 02149
Attn: Dr. J. O. Smith

North American Aviation Co.
S & ID Division
Downey, California 90241
Attn: Dr. James Nash

Oklahoma State University
Stillwater, Oklahoma 74075
Attn: Prof. William L. Hughes
        School of Electrical Engineering

Paul Howard Associates Inc.
Centerville, Maryland 21617

Power Information Center
University of Pennsylvania
3401 Market St., Rm. 2107
Philadelphia, Pennsylvania 19104

Power Sources Division
Whittaker Corporation
9601 Canoga Avenue
Chatsworth, California 91311
Attn: Dr. M. Shaw

Prime Battery Corp.
15600 Cornet Street
Santa Fe Springs, California 90670
Attn: David Roller

RAI Research Corp.
36-40 37th Street
Long Island City, N. Y. 11101

Radio Corporation of America
Astro Corporation
P. O. Box 800
Hightstown, New Jersey 08540
Attn: Seymour Winkler

Radio Corporation of America
AED
P. O. Box 800
Princeton, New Jersey 08540
Attn: I. Schulman

Radio Corporation of America
415 South Fifth Street
Harrison, New Jersey 07029
Attn: Dr. G. S. Lozier
        Bldg. 18-2

Southwest Research Institute
8500 Culebra Road
San Antonio, Texas 78206
Attn: Library

Sonotone Corporation
Saw Mill River Road
Elmsford, New York 10523
Attn: A. Mundel

Texas Instruments, Inc.
P. O. Box 5936
Dallas, Texas 75222
Attn: Dr. Isaac Trachtenberg

TRW Systems, Inc.
One Space Park
Redondo Beach, California 90278
Attn: Dr. A. Krausz, Bldg. 60, Rm. 147

TRW Systems, Inc.
One Space Park
Redondo Beach, California 90278
Attn: Dr. Herbert P. Silverman

TRW, Inc.
23555 Euclid Avenue
Cleveland, Ohio 44117
Attn: Librarian

Tyco Laboratories, Inc.
Bear Hill
Hickory Drive
Waltham, Massachusetts 02154
Attn: Dr. A. C. Makrides

Unified Sciences Associates, Inc.
826 S. Arroyo Parkway
Pasadena, California 91105
Attn: Dr. S. Naiditch

Union Carbide Corporation
Development Laboratory Library
P. O. Box 5056
Cleveland, Ohio 44101

Electromite Corporation
Attn: R. H. Sparks
  General Manager
562 Meyer Lane
Redondo Beach, California 90278

Union Carbide Corporation
Parma Laboratory
Parma, Ohio 44130
Attn: Dr. Robert Powers

University of Pennsylvania
Electrochemistry Laboratory
Philadelphia, Pennsylvania 19104
Attn: Prof. John O'M. Bockris

Westinghouse Electric Corporation
Research and Development Center
Churchill Borough
Pittsburgh, Pennsylvania 15235

Whittaker Corporation
3850 Olive Street
Denver, Colorado 80237
Attn: J. W. Reiter

Whittaker Corporation
Narmco R&D Division
3540 Aero Court
San Diego, California 92123
Attn: Dr. M. Shaw

Yardney Electric Corporation
40 Leonard Street
New York, New York 10013
Attn: Dr. Geo. Dalin